

**Prediction modelling of Land Use/Land Cover changes and its
impact on Urban Heat Island intensity over the Greater Kovai
Region: A Geomatics Approach**

Thesis submitted to Amrita Vishwa Vidyapeetham in partial fulfilment
of the requirement for the degree of Master of Science in
Environmental Science with a minor in Remote Sensing &
Geographical Information System



Submitted by:

JEEVAN.M. P

AM.PS.P2ENV23007

Under the supervision of

DR. ARUN P R

Senior Scientist and Head i/c

Work carried out at the Department of Hydrology and Climatology Group

KSCSTE-Centre for Water Resources Development and Management

Kunnamangalam, Kozhikode- 673571

Kerala, India

June, 2025





KSCSTE-CWRDM

KSCSTE - CENTRE FOR WATER RESOURCES DEVELOPMENT AND MANAGEMENT

ജലവിവേ വികസന വിനിയോഗ കേന്ദ്രം



An Institution of Kerala State Council for Science, Technology & Environment, Govt. of Kerala
കേരള ശാസ്ത്ര സാങ്കേതിക പരിസ്ഥിതി കമ്മീറ്റിൽ സ്ഥാപനം, കേരള സർക്കാർ

Dr. Arun P.R.

CERTIFICATE

This is to certify that this dissertation entitled "Prediction modelling of Land Use /Land Cover changes and its impact on Urban Heat Island Intensity over the Greater Kovai Region: A Geomatics Approach" is a bonafide record done by Mr. Jeevan M.P. (Roll No: AM.PS.P2ENV.23007), in partial fulfilment of the requirement for the Degree of Master of Science in Environmental Sciences with a minor in Remote Sensing and GIS of Amrita Vishwa Vidyapeetham, Amritapuri Campus was carried out during Jan - May 2025, at the Centre for Water Resources Development and Management (CWRDM), Kozhikode, Kerala, under my guidance and supervision. To the best of my knowledge, the work reported by him, does not form part of any other thesis or dissertation on the basis of which a degree or award was conferred on an earlier occasion on this or any scholar.



Dr. Arun P.R.
Senior Scientist & Head
Hydrology and Climatology Research Group
Centre for Water Resources Development and Management (CWRDM)

Kozhikode, Kerala, India, 673 571

Mob: +91 8547463754

Office: 0495 2351821

arun@cwrdm.org

May, 2025



DECLARATION

I, Jeevan. M.P, hereby declare that the project entitled "**Prediction modelling of Land Use/Land Cover changes and its impact on Urban Heat Island intensity over the Greater Kovai Region: A Geomatics Approach**" is the original work done by me under the supervision and guidance of Dr. Arun P R for the partial fulfilment of the requirements of the award of degree, Master of Science in Environmental Sciences with a Minor in Remote Sensing & Geographical Information Systems (RS & GIS) of Amrita Vishwa Vidyapeetham, Amritapuri Campus during 2023-25.

Place: Amritapuri

Jeevan. M. P

Date: 09/06/2025

(AM.PS.P2ENV23007)

Approved by:

Dr. Sreedha Sambhudevan, Chairperson,

Department of Chemistry, Amrita School of Physical Sciences

Amrita Vishwa Vidyapeetham, Amritapuri Campus

Clappana (P. O.), Kollam, Kerala – 690 525

ACKNOWLEDGEMENT

Firstly, I would like to express my deepest gratitude and praise to God Almighty for blessing me throughout my life and especially during my project to enable me to accomplish it as planned.

I am very grateful to my guide, **Dr. Arun P R**, Senior Scientist & Head i/c, KSCSTE-Centre for Water Resources Development and Management, for their invaluable advice, continuous encouragement, and unwavering faith in my abilities throughout this project. Their expertise and insights have been instrumental in shaping this work.

I wish to thank Dr. **Sreedha Sambhudevan**, Head of the Department of Chemistry, who gave me an opportunity.

I am also grateful to my Lecturers, **Dr. Smitha Chandran S**, **Dr. MS Shylesh Chandran**, and **Dr. Sumith Satheendran**, and others for their insightful comments and suggestions during the development of this research.

List of Figures

SL No.	Figure	Page No.
1	Study area of the Greater Kovai Region	21
2	Methodology of Workflow	23
3	LULC of 2016	29
4	LULC of 2020	30
5	LULC of 2024	31
6	LULC of 2028	32
7	LULC of 2032	32
8	Graphical representation of LULC change dynamics	34
9	LST of 2016	35
10	LST of 2020	36
11	LST of 2024	36
12	Predicted LST of 2028	37
13	Predicted LST of 2032	28
14	LST Class Area Comparison over Time	39
15	UHI Intensity of 2016	40
16	UHI Intensity of 2020	40
17	UHI Intensity of 2024	41
18	Predicted UHI Intensity of 2028	42
19	Predicted UHI Intensity of 2032	42
20	UHI Intensity Comparison Graph	43
21	Total percentage area of each LULC class in 2016	44
22	Total percentage area of each LULC class in 2032	45
23	Area under <35°C	46
24	Area under >35°C	47

List of tables

SL No.	Table	Page No.
1	Time of Data Acquisition	22
2	Definition of Land Classes	24
3	UHI Intensity Ranges	26
4	Overall accuracy and Kappa coefficient	28
5	Area and Percentage of LULC	33
6	LST Class ranges	34
7	LST area zones	38
8	UHI Intensity area	43
9	Comparison of Air and Surface Temperature	45
10	Average LST of each Land Class	46

Contents

SL No.	Title	Page No.
1	ABSTRACT	8
2	INTRODUCTION	9
3	OBJECTIVES	14
4	REVIEW OF LITERATURE	15
5	METHODOLOGY	20
6	RESULTS	28
7	DISCUSSION	44
8	CONCLUSION	48
9	FUTURE PERSPECTIVES	49
10	REFERENCES	50

1. ABSTRACT

The rise in urbanisation has caused many effects on the surrounding environment, coupled with the warming has raised the temperature through climate change. These conditions have caused the occurrence of the Urban Heat Island effect. The changes in LULC can significantly affect the LST, thereby amplifying the impact of Urban Heat Islands intensity. In this study, the Greater Kovai region was taken as an example to learn the effects of the land dynamics. The Landsat satellite imagery was taken at a similar time interval. The LULC classification was done through a machine learning technique. The LST was also extracted from the satellite imagery through the process of the split-window algorithm. The UHI intensity was also calculated with the help of LULC and LST. Based on the values, the UHI intensity classes were categorised into five (very low to very high). For the prediction of LULC, LST, and the UHI intensity, the CA-ANN (Cellular Automata- Artificial Neural Network) model from the QGIS software was used to predict the conditions for 2028 and 2032. The findings found that there is a strong link between LULC and LST. The vegetation and water bodies had a much lower LST compared to Bare land and Built-up. The projections suggested an increase from 14% in 2016 to 18 % in 2032. The model also predicted an increase in the area under the above 40°C zone from 156 sq. km to 235 sq. km. The forecasted UHI intensity also had some notable changes. The model predicted a brief cooling where the area under the “Low” category had increased, however the area under the “Moderate” and “High” zones experienced an increase with the help of this analysis, various stakeholders and government officials to plan further urban development in a sustainable way and also adopt mitigation strategies to control Urban Heat Islands.

2. INTRODUCTION

The Urban Heat Island (UHI) refers to a localised phenomenon where urban centres undergo considerably elevated temperatures than the adjacent or peripheral non-urbanised areas, such as suburbs (O’Malley C., 2014). The Urban heat island effect is a particularly significant manifestation of climate change observed in the current decade (Han et al., 2023). Typically, within major metropolitan areas, the temperature in the central urban zone is elevated compared to that in the outlying or suburban regions (Nuruzzaman, 2015). The changes seen in the environment can cause the effect of urban heat, which may arise from the reduction of vegetation, evaporation of water, presence of dark objects that can absorb heat and also from anthropogenic activities (Mohajerani et al., 2017). It is making people difficult to walk outside due to the effects of climate change, urban heat islands, and the change in energy balance seen in cities (Hayes et al., 2022). There is a temperature difference seen in both urban and rural areas, especially during the nighttime, meaning the effect of urban heat islands is observed during the dark (Taslim et al., 2015). The emissions of GHG into the atmosphere have caused significant changes in the climate globally (Sachindra et al., 2016).

Surface and Atmospheric urban heat islands are the two types of urban heat islands (Kikon et al., 2016). With the help of thermal remote sensing, the SUHIS (Surface urban heat islands) can be obtained, as it is the temperature difference between the urban and rural zones of the area (Voogt & Oke, 2003). Both the Urban canopy and boundary layer (UCL & UBL) can be estimated by various ground based and vehicle mounted sensors (Hu & Brunsell, 2015). According to the WHO, the 2003 European heat wave caused significant mortality, with 14,802 deaths recorded in France, 2045 deaths in the UK, and 2099 deaths in Portugal (Cao et al., 2019). A World Bank study predicts that by 2030, developing countries will see their cities with populations of 100,000 or more triple their urbanised land area, developed countries are also projected to experience significant growth, with cities expanding by 2.5 times, even with lower population numbers and growth rates (Angel et al., 2005).

Human activities have converted or substantially changed roughly fifty per cent of the ice-free land on Earth during the last 10,000 years (Lambin et al., 2003). Changes in land use and land cover are a major factor driving alterations in the Earth’s systems, especially climate (Verburg et al., 2011). Land use and land cover change influence not only GHG emissions but also climate-relevant properties of the land surface (Verburg et al., 2011). The influence of land use and land cover change on climate change is primarily examined by considering land use/cover

change as a cause of climate change (Schulp et al., 2008). More areas of land are experiencing drastic changes everywhere in the world (Mas, 1999).

Ventilation, surface roughness and radiative balance are some of the factors that influence surface temperature (Zhang et al., 2009). The dense and taller buildings cause thermal anisotropy (Voogt & Oke, 2003). LST is higher when there is rapid urbanisation, loss of vegetation cover, and increase of impervious layer on the ground (Morris et al., 2017). Built-up areas which are less spaced, trap a lot of heat and also restrict the movement of wind during hot weather (Morris et al., 2017). Higher levels of LST are observed in high density building areas (Oleson et al., 2015). Low reflectivity materials has the ability to take in solar radiation, thereby increasing the LST (Moghbel & Shamsipour, 2019).

During day time the heat is trapped in the built-up areas (Shahmohamadi, Che-Ani, Etessam, et al., 2011). Materials that are low in reflectivity are one of a major cause for the UHI effect (Shahmohamadi, Che-Ani, Maulud, et al., 2011). The difference in the surface properties in urban and rural zones contributes to higher UHI levels (C. Li & Zhang, 2021). Some areas undergo low albedo effect due to its impervious nature which causes evaporation and heat absorption (Y. Li et al., 2020). For developing urban area, materials having low reflectivity are used which can contribute to high UHI (Koç et al., 2022). The temperature difference seen between urban and rural areas resulted from the properties of urban materials like roads, concrete (Shahmohamadi et al., 2010). In temperate zones, when the impervious layer replaces vegetation the heat storage capacity increases, as well as the brown ratio (Zipper et al., 2017).

The lack of vegetation in urban areas leads to less evapotranspiration (ET), which means less latent heat is used, leaving more energy to increase sensible heat and thus temperatures (Small et al., 2020). Cities show a strong link between the amount of paved or built-up surfaces and how hot the ground gets, with streets being particularly prone to higher temperatures (Small et al., 2020). Impervious asphalt, a common material for traditional pavements, can reach very high surface temperatures, typically between 65 and 80 °C during hot summer months. The quality of air and water has decreased due to the effect of high air temperature, which also led to the use of more energy (Manteghi, 2020). Some findings indicate that the taller buildings contribute to higher levels of LST and UHI effect (Liapopoulou & Heo, 2013). Densely built tall buildings along the street has a major impact on UHI (Grifoni et al., 2013). The modifications caused in the urban area can either rise or stabilise the temperature gradient (Nakata-Osaki et al., 2015). Excessive alterations caused to the land and other human activities

are a leading factor to develop these effects (Feng et al., 2012). The warmest places are typically seen in the city centres of a metropolitan area, where the UHI effect is normally high (Shahmohamadi, Che-Ani, Etessam, et al., 2011). Factors like climate, population and the effects of factories influence the amount of heat dispersed into the atmosphere (R. Liu & Han, 2016). High air temperatures can cause an increase in cooling demand, particularly in hot climates (Vardoulakis et al., 2013).

The effect of UHI can induce a rise in energy levels to cool the buildings and lower it lowering it for heating (X. Li et al., 2019). Many studies also suggested that the UHI effect can lead to higher energy consumption and high levels of heat-related deaths (Shi et al., 2019). Low albedo, impermeable materials, poor ventilation, and anthropogenic heat can lead to positive thermal balance and the amplification of the UHI effect (Kubilay et al., 2020). In Arizona's hot summers, urbanisation, by increasing impervious surfaces, diminishes outdoor thermal comfort, directly causing greater energy consumption for space cooling, especially during the summer months (Tewari et al., 2017).

UHI effects, exhibiting significant temperature variations across seasons, particularly during dry and calm weather, substantially influence the specific energy demands of buildings in localised areas (Yi & Peng, 2017). Urban buildings with 13% higher air conditioning energy consumption contribute to greater waste heat, thereby elevating the urban heat island effect (Baniassadi et al., 2018). Elevated energy use in cities intensifies the Urban Heat Island (UHI) effect by releasing more heat, leading to warmer urban centres, particularly at night, because of stored heat and freed by surfaces like asphalt and buildings (Garuma, 2022). The Urban Heat Island effect, with its higher temperatures in cities, worsens air pollution by exacerbating atmospheric conditions that diminish air quality, thereby creating further environmental difficulties for urban centres (J. Yang et al., 2015). The capacity of the Urban Heat Island (UHI) effect to worsen air pollution in urban areas intensifies health risks for city populations, a relationship between higher temperatures and declining air quality is recognised as a key way the UHI effect undermines public health (Heaviside et al., 2017).

The effect of UHI also has negative impacts on human health as it may worsen air pollution and increase the ozone concentration because of maximum temperatures (Heisler & Brazel, 2015). The UHI can also affect air pollution by factors like mixing temperature and layer, and how they are spread out and accumulated (Swamy et al., 2017). Studies in the U.S. indicate that when the boundary layer is suppressed, pollutants tend to stay closer to the ground.

Additionally, models reveal a strong link between temperature and VOC emissions and higher levels of both ozone and fine particulate matter (PM2.5), particularly in urban and coastal areas (Swamy et al., 2017). UHI-related temperature increases can alter the timing of plant development, like when leaves appear and change colour, both within urban areas and in their surroundings (Zipper et al., 2016). Extended periods of very high temperatures can result in sickness and death linked to heat, particularly during heat waves and in cities where urbanisation causes even hotter conditions (Lee et al., 2017).

The 2007 heat wave in Japan, which tragically caused 904 deaths from heat stroke, highlights the deadly potential of heat-related fatalities during severe weather conditions (Lee et al., 2017). The influence of weather on human health has gained considerable importance lately, particularly when considering the possible effects of global warming and the intensified urban heat island effect resulting from city growth (Tan et al., 2010). It seems that city dwellers, young children, older adults, individuals with ongoing illnesses or disabilities, and those residing in urban settings that amplify local heat during heatwaves face the most significant dangers (Loughnan et al., 2012). Individuals who already have heart-related illnesses face a greater chance of dying or becoming sick due to heat (Loughnan et al., 2012). Common illnesses directly caused by heat, like rashes, cramps of the skin, fainting from heat, and heat stroke, can quickly become fatal if medical help isn't received promptly (Dong et al., 2014).

Research has also indicated that elevated temperatures might worsen illness and increase death rates associated with diseases of the heart, lungs, blood circulation, kidneys, and nervous system (Dong et al., 2014). The UHI effect also presents the danger of heat stress-related injuries, which can jeopardise the well-being of people living in cities (Shahmohamadi, Che-Ani, Etessam, et al., 2011). The expansion of built-up and impermeable surfaces due to urbanisation intensifies UHIS, and this urban growth can manifest through infill, extension, or leapfrog developments (Tran et al., 2017). Urbanisation entails land use and land cover changes where natural ground and plants are replaced by impermeable surfaces, farming, businesses, factories, and low buildings are substituted with tall urban structures, leading to the substitution of natural materials with artificial constructions that change the local climate and alter land surface temperature (Khan et al., 2020). With half the world's population currently residing in urban areas, and this number is projected to jump up in 2050, natural resources and habitats face escalating pressure due to this swift population expansion (Karakuş, 2019). As a result of Land Use/Land Cover (LULC) changes in urban areas, natural surface conditions has been modified, and causing the energy and water balance of the atmosphere above (Harmay et al.,

2021). The land's physical characteristics and climate are influenced by the changes in LULC (Harmay et al., 2021).

Most of the vegetation are replaced by impervious surfaces during the past 50 years, causing environmental degradation all over the world (Dissanayake et al., 2019). Urban growth and urban sprawl have an impact on the increase of high LST (P. Liu et al., 2020). The UHI intensity is affected due to the loss of green cover (Atasoy, 2019). Global warming and climate change are observed due to the conversion of natural land into other land classes like settlements (Pramanik & Punia, 2020).

The green cover has the ability to mitigate the effect of UHI intensity as the number of urban areas increases (B. Yang et al., 2015). The UHI intensity has a negative impact on water bodies when compared to other classes (B. Yang et al., 2015). The way how streets are connected and how the built-up areas are laid out, and how much impervious layer are seen can either accelerate or decelerate the effect of it (Erdem et al., 2021). With the help of RS, we are able to calculate the LST of the area by considering the relative radiance, brightness and emissivity (de Almeida et al., 2021). Satellites such as Landsat and MODIS are commonly used for LST extraction (de Almeida et al., 2021). The temperature records from both thermal IR and weather stations are used to estimate the UHI effects (Favretto, 2018). Combining satellite data with ground truth data can significantly provide us with better results for further investigation (Mohan et al., 2013). GIS can help in learning about temperature over a large area (Merbitz et al., 2012).

3. OBJECTIVES

- Analyse LULC changes in the Greater Kovai region
- Estimate LST distribution across the study area
- Calculate the UHI intensity, in relation to LULC and LST
- Predict the LULC, LST and the UHI Intensity for 2028 and 2032 by using the CA-ANN model
- Compare the differences during the study period (2016 to 2032)
- Represent the data visually by maps and graphs.

4. REVIEW OF LITERATURE

A study in Ibadan, Nigeria, was done to learn the connection between LULC and LST, with the help of Landsat images and GEE platform. Higher levels of LST are seen in built-up areas (Fashae et al., 2020).

A study in Beijing was carried out to understand the link between LULC and LST, satellite images were downloaded from 1995 to 2000 and was found that the urban areas underwent high LST and Low in green areas (Jiang & Tian, 2010).

The impervious layer has a positive impact on the LST. LULC mapping was done with the Landsat image and the MLC method (Celik et al., 2019).

The impact of urbanisation is studied in Jeju Island, South Korea. This was achieved by using Landsat imagery and supervised classification methods. In the analysis, the urban area has increased by doubled, along with a decrease in barren land. LST data showed that there is a correlation with urban areas. The temperature increased from 2.47 °C to 3.10 °C during the study period (Moazzam et al., 2022).

To find the link between LULC and LST a study was conducted in Monsaura, Egypt. The study also estimated the effect of UHI with the help of satellite imagery from 1991 to 2021. Furthermore, CA and ANN models were used to predict the future LULC and LST of 2031. The study found a positive correlation with NDBI and a negative correlation with NDVI. The prediction also suggested that there will be 20% increase in urban areas and an 18% decrease in vegetation (Sameh et al., 2022)

Both Landsat and MODIS satellites were used to identify the impacts caused due to LULC change, LST and UHI effect. ML models like linear regression, Random Forest were used for the study. The analysis revealed that there is a 70% increase in urban areas and a 62% decrease in dense vegetation in the study area. The increase in surface UHI was also apparent (Rees et al., 2024).

Landsat images from 1900 to 2018 were taken in Bangladesh to study the impacts of LULC on LST. It was found that there was an increase in urban areas, but the agricultural land remained the same. Other land classes, such as water bodies, vegetation, recorded lower temperatures. The effect of UHI was maximum during the year of 2018 (Akter et al., 2021).

LULC classification and LST calculation was done using Support vector mechanism and mono-window algorithm to identify the effects of UHI. The study was done in Beijing, China. The study revealed an increase of LST and UHI. This is due to an increase in the impervious surface areas and also a decrease in farm lands. Areas like bare soil and rooftops have experienced higher levels of LST (Ding & Shi, 2013)

In a study done in Iraq, the LULC and LST data was derived from Landsat imagery, taken from 1990, 2000, and 2016. The findings indicated higher levels of LST in the urban and barren areas, while the forest and water bodies showed lower levels of LST. The NDBI, NDVI, and the NDWI were created to find any correlation (Ibrahim, 2017).

Urban-rural gradient analysis indicated an increase in mean land surface temperature by 2-3°C at the heart of the city and 5-7 °C at the boundary. The impervious surface layer also recorded higher temperature differences compared to other land classes, such as water and vegetation. Correlation analysis showed an overall negative relationship between LST and the Normalised difference vegetation index and a positive relationship with the Normalised difference built-up index (Rousta et al., 2018)

A study was aimed to predict the future changes in the LULC of the fastest-growing city in Bangladesh, Chattogram. The prediction was done with the help of CA and ANN. The forecast showed that there is an increase in built-up area by 9-14%, while the green areas decreased by 8-12% by 2029 and 2039. The predicted LST also shows that more areas will experience higher temperatures (26-36 °C) (Kafy et al., 2021).

With the help of models like CA-ANN, the projection for LULC 2053 was done. This study was done in Henan, China. The urban areas and the water bodies will increase, and the barren land will decrease. Sarfo et al.'s (2024) A similar study was done in Karachi, where this model was used to predict LULC. The results indicated a major increase in Urban area and a decrease in other land classes (Din & Yamamoto, 2024).

The LULC and LST for 2025 and 2030 are predicted using CA-ANN and XGBoost regression models. The UHI was also calculated with the help of projected findings. There was an increase in built-up and a decrease in vegetation in 2030. The LST also increased in 2030 (Mohammad et al., 2022).

Between 2001 and 2010, the urban areas increased rapidly in New Delhi. The DTR decreased from 12°C to 10°C, which became evident due to growing urbanisation (Mohan & Kandy, 2015)

The association among LULC and LST and the UHI effect is analysed in the area of Kamrup in Northeast India. Machine learning models were used for the study. The prediction is done for LULC and LST using the CA-ANN model. The forecast indicated a major increase in urban area and also the LST (Choudhury et al., 2023).

The effect of LST due to urbanisation is studied in Ernakulam, Kerala during 2005 to 2020. The findings revealed that the vegetation has reduced from 47% to 29%, and an increase in built-up, 6% to 15%. Correspondingly, LST increased by 2.55 °C for vegetated land and 4.82 °C for built-up land, with an overall district temperature rise of 3.45 °C (Vohra et al., 2024).

A study analysed the effect of LULC changes on LST in Bhubaneswar City, Eastern India, using Landsat data and machine learning from 1991 to 2021. The findings indicated a large increase in mean LST. This is due to rapid urbanisation and shows a positive correlation. Likewise, there was a significant loss in green space over the 30 years. In 1991, the dominant land class was agricultural land, but in 2021, the dominant land class was built-up areas (Das et al., 2022).

A study by (Verma & Garg, 2021) was done to analyse the relationship between the LULC changes and the UHI effect in Lucknow, India, during the years 1985 to 2015. The relation between LULC and LST was investigated. The LST was calculated. The correlation between NDVI and NDBI was also noted.

The north and south part of Raipur was examined to learn the effects of UHI in urban and rural areas. Some parts of the area had shown high levels of UHI (Guha et al., 2020).

The link between LULC and LST are studied to find any relation. The impervious surface had a great influence on the LST. There was some increase in temperature both in summer and winter (Gupta et al., 2020).

Almost 50% of the total land was the cause of the overall warming of the area. There was some difference in temperature from 2001 to 2010 (Gogoi et al., 2019).

Vegetation decreased up to 13 square km. Due to this, there was an increase of 1.5°C in LST. A positive correlation was seen between NDBI and LST in urban areas, supporting the link between LST and urbanisation (Dhar et al., 2019).

A paper by (Bagyaraj et al., 2023) explores the LST and UHI effect with the help of satellite data from 1988 and 2021 in the region of Kancheepuram district, Tamil Nadu. Here, the effect of surface temperature is analysed using LULC changes. RS techniques are used to identify the LULC changes and also the changes in LST. The mean LST ranges from 14-31 °C in 1985, 25-39 °C in 2005, and 31-47 °C in 2021, showing a 152% increase over the four decades. Urban areas, especially parking lots, showed maximum UHI effect, and vegetated areas showed less effect; this may be due to the properties of construction materials.

A study by (Balsubramanian et al., 2021) analysed the connection between LULC changes and LST in the coastal area of Ramnathapuram using Landsat images from 2000 to 2020. The study indicated an increase in built-up areas from 8 km² to 44 km² from 2000 to 2020. The study also observed maximum LST of 30 °C, 29 °C, 30 °C, 30 °C, 27 °C for the years 2000, 2005, 2015, 2020, respectively.

Due to the rapid rise in urbanisation in the region of CMA (Chennai Metropolitan area), the LULC change was examined to learn its impact on LST and UHI. The analysis suggests that natural land cover was converted into settlement areas. The peri-urban areas increased from 56 to 73%. The high effect of UHI are seen in newly converted urban areas (Muthiah et al., 2022)

The LST in the South Chennai region was analysed to find a correlation among NDVI and NDBI. The areas where there are more barren and built-up land was found to have high LST levels, whereas the vegetation and water bodies showed lower levels of LST (Narayani & Nagalakshmi, 2024).

The effect of UHI is studied in Chennai during the years 2000 to 2020. Urban areas had a powerful link with built-up areas and a negative response to greener areas. The correlation between NDBI and NDVI are also studied (Faizan, 2020).

The estimation of LST was studied from 2015 to 2020 in Coimbatore. The authors have found that there is an increase of 1 °C in maximum temperature. The minimum LST also increased from 15 °C to 19 °C during the study period (Aravind et al., 2022).

(Palanisamy et al., 2021)'s study identified urban heat zones in Tiruppur Corporation, Tamil Nadu. The study investigates the spatiotemporal patterns of LULV, LST, NDVI, NDBI, and

UTFVI with the help of Landsat and Sentinel images for 1991, 2001, 2011, and 2021. Support Vector Machine was used for the LULC classification.

Analysing LULC changes and their impact on LST in the Chennai Metropolitan Area (CMA) from 2000 to 2020 using Landsat imagery with high-accuracy LULC classification. The future prediction for LULC and LST for 2030 and 2040 was also done using ANN and cellular automata. It reveals a major decrease in agricultural and forest land, along with a significant increase in built-up areas. Future prediction also indicates continued loss of natural area and expansion of urban areas (Faizan & Hudait, 2024).

(Ghosh & Porchelvan, 2018) ‘s study examined the bond between LST and LULC in Vellore district, Tamil Nadu, using Landsat 7 imagery. The study revealed that urban and heavily populated areas exhibited higher temperatures (35-43 °C), while the forest areas observed lower temperatures (13-27 °C).

(Marianne Rhea & Thangaperumal, 2023)’s study analysed the impact of urbanisation on LULC and LST in Madurai district, Tamil Nadu, India, using Landsat images from 2003, 2011, and 2019. The results indicated a 50% decrease in water bodies and an increase in barren land, resulting in higher levels of LST. There were also changes in built-up and vegetation.

5. METHODOLOGY

Study area

The present study focuses on the greater Coimbatore (Kovai) region in the western part of Tamil Nadu. This fast-growing urban landscape consists of heavily populated zones and surrounding semi-urban and rural areas. As illustrated in Fig., the study area includes key locations such as Coimbatore city, Pollachi, Sulur, Singanallur, Madukkarai, Aninsahi, and parts of Tiruppur.

This region lies approximately between 10.5° N to 11.3° N latitude and 76.7° E to 77.2° E longitude, spreading outward from the city centre by about 17 to 20 kilometres in various directions. The study area covers around 1,200 square kilometres, which includes a diverse range of land uses including urban settlements, fallow lands, industrial zones, vegetation, and some mountain ranges. Topographically, the terrain is mostly flat, though it gradually rises towards the foothills of the western Ghats on the western and southern fringes. Notable elevations near areas like Melmudi, Sundakkamuthur, and Madukkarai (Fig.1) introduce a calm climate, making the region an interesting case for environmental and urban studies.

Coimbatore experiences a semi-arid climate, with hot, dry summers and moderate monsoon rainfall. The UHI effect is prone to such conditions. The distribution of heat due to the changes in LULC can be examined by analysing the urban and rural areas. The forecast of the LULC and UHI relationship can be investigated by these conditions.

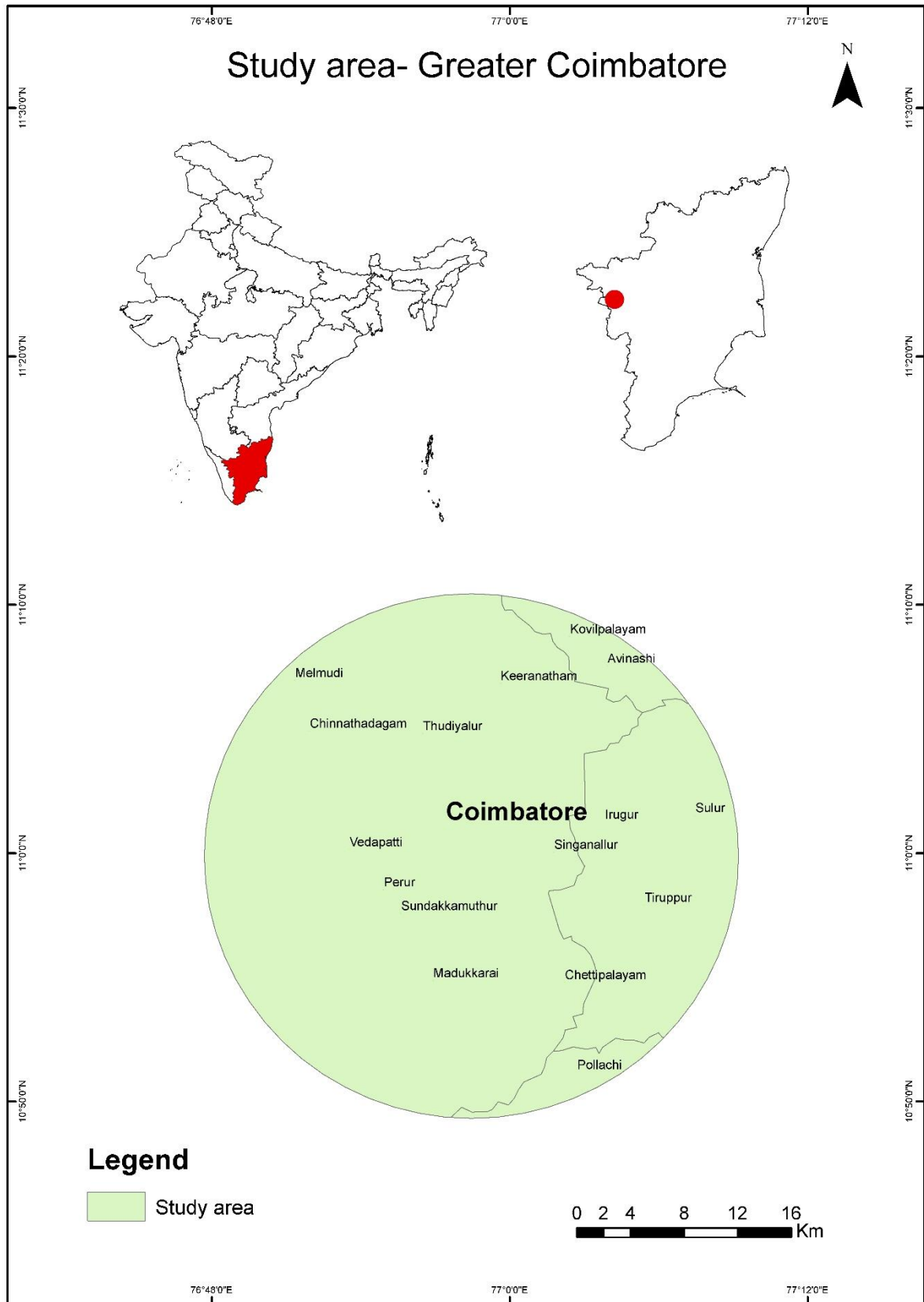


Fig.1: Study area of the Greater Kovai region

Data collection

Landsat data is very effective for calculating the Land surface temperature and also for UHI studies (Aslan & Koc-San, 2016). It has very detailed data, which is ideal for land cover mapping (Knorn et al., 2009). They are found to be cost-effective and easy to interpret (Knorn et al., 2009). It has become very convenient to map LULC over a large area, as well as to monitor the changes (Giniyatullina et al., 2014). Since the satellite visits the same area in a period of 16 days, we are able to see the changes in the land over a period of time (Capolupo et al., 2020). Even though there are only single snapshots from single days, the stable temperature and humidity levels across those times give us a good understanding of how the urban heat island effect is spread out during different periods when the weather is behaving similarly (Xiang et al., 2024). The data are collected from the USGS database. As depicted in the Table. 1, the satellite imagery was taken in four-year gaps, utilising the Landsat 8 satellite image. The images are taken from a similar time frame to get accurate results. These dates were chosen because they fall within the same season and have clear skies. This helped in reducing the influence of changing weather, like clouds or rain, and how the results are calculated.

No.	Landsat satellite	Acquisition date	Acquisition time	Path- row number
1	Landsat 8 OLI_TIRS	2016-03-20	05:11:03 GMT	144/52
2	Landsat 8 OLI_TIRS	2020-03-31	05:10:58 GMT	144/52
3	Landsat 8 OLI_TIRS	2024-03-26	05:10:54 GMT	144/52

Table 1: Time of Data Acquisition

Along with the satellite images, some independent variables like slope, proximity to roads, buildings, and water bodies are also collected. The DEM (Digital Elevation Model) was taken from ISRO's Bhoothnath database, and the proximity to roads, settlements, and water bodies is extracted from the OpenStreetMaps database. These variables are important as it is used as input variables in the MOLUSCE plugin in QGIS for forecasting the resulting land cover changes, surface temperature, and urban heat island intensity. The methodology is illustrated as a flow diagram in Fig. 2

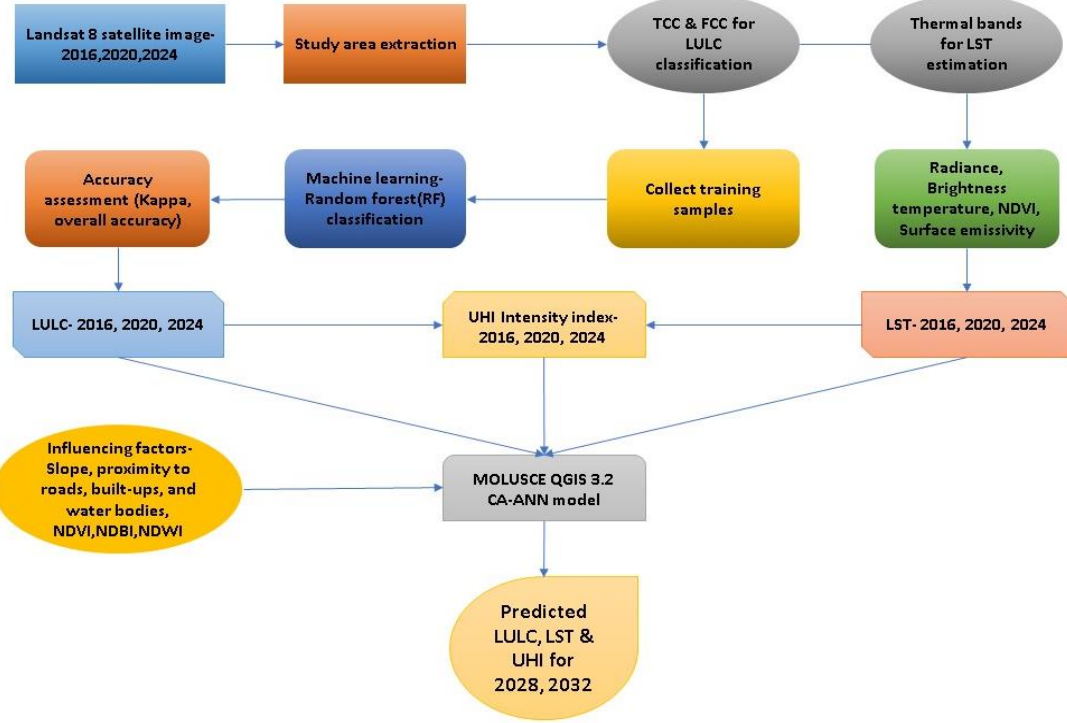


Fig.2: Methodology of Workflow

LULC classification

Based on the study area, the land classes were divided into six classes: barren land, fallow land, Vegetation, built-up, water, and forest-mountain. The basis of the classification is described in the table. Barren land refers to the area which have bare soil, less to no vegetation, sand, and dry patches. Fallow land consists of land which are already cultivated and left as fallow, or unused. Vegetation includes areas that are green with trees, shrubs, grasslands, and croplands. Built-up area represents urban infrastructure like buildings, roads, and indicates human modifications (Table 2). The mountains and water bodies are very essential land classes for environmental balance and are also found to have lower temperatures compared to the other land classes. Various methods like ground surveys and satellite imagery have helped researchers to map the different land use and land cover maps, and also to track the changes (Talukdar et al., 2020).

Different satellites like Resourcesat, MODIS, IRS, ASTER are used to map the Land use/ Land cover changes as well as to predict the future changes (Talukdar et al., 2020). The most basic method to classify LULC is done by examining the satellite images and classifying them using supervised or unsupervised algorithm methods (Avci, C et al., 2023). In the current day, many machine learning models like Random Forest (RF), support vector machine (SVM) are used to classify LULC in a more effective and accurate manner (Avci et al., 2023).

Random Forest works by creating a multitude of decision trees, essentially a ‘forest’, each tree learns from a slightly different, randomly selected portion of the original data, figuring out the best way to split information by looking for the most organised patterns (Thonfeld et al., 2020). The RF works based on the number of votes received in a single category, the category which receives the most votes will be the final result (Kasahun & Legesse, 2024). Out of all the other models, the Random Forest had the highest accuracy, showing that it can classify the LULC effectively and accurately (Zhao et al., 2024). In this specific study, the Random Forest model was used for the LULC classification, the Google Colab platform was used to map and also provide accuracy data.

Land cover	Instruction
Barren land	Bare soil, dry vegetation, rocky land, sand
Fallow land	Cultivated agricultural land
Vegetation	Trees, shrubs, grasslands, croplands
Built-up	Urban area, roads, and an airport
Water	Rivers, ponds, and water bodies
Forest- Mountains	Elevated areas, forests, dense vegetation

Table 2: Definition of Land Classes

Estimation of LST

The temperature that is felt on the ground when touched, or in other words, the temperature felt on the surface of Earth, is known as Land Surface Temperature (LST) (Rajeshwari & Mani, 2014). Due to the rise in GHG, LST has increased more, affecting the glaciers and polar caps (Rajeshwari & Mani, 2014). Both natural and human activities are major causes for the effects of high LST (Rajeshwari & Mani, 2014). A split-window algorithm is been used to calculate the LST. It is a step-by-step process by which the TOA, BT, NDVI, Land surface emissivity and then the LST are calculated systematically by GIS software.

Top of atmospheric spectral radiance (TOA)

The ability of the surface to reflect solar waves in known as TOA (Aravind et al., 2022). The TOA is calculated by the linear scaling of band values (Rajeshwari & Mani, 2014).

$$L\lambda = M_L * Q_{cal} + A_l \text{ (USGS, 2023)}$$

$$Eq. 1$$

Where $L\lambda$ is the TOA, M_L is the Multiplicative rescaling factor, Q_{cal} is the band, and A_l is the rescaling factor.

Brightness temperature (BT)

The BT is the measure of microwave radiation that is emerged from the Earth's atmosphere, which is similar as the temperature of a black body releasing a similar radiance (Aravind et al., 2022). The equation is given as:

$$BT = K_2 / \ln((k_1 / L\lambda) + 1) - 273.15 \quad Eq. 2$$

Here, k_1 and k_2 represent TIRS thermal constants, and $L\lambda$ denotes TOA.

Normalised Difference Vegetation Index (NDVI)

The Normalised Difference Vegetation Index (NDVI) is a measure of vegetation greenness and health, calculated using the reflectance values from the near-infrared (NIR) and red bands of satellite imagery (Xiang et al., 2024).

$$NDVI = (NIR - RED) / (NIR + RED) \quad Eq. 3$$

Where NIR is the DN value of band 5, and RED is band 4

Land surface emissivity

Surface emissivity, also referred to as land surface emissivity, quantifies how effectively a surface emits thermal radiation compared to a perfect blackbody at the same temperature and wavelength (Xiang et al., 2024). Land surface emissivity, representing the average radiative efficiency of the ground, is often estimated using vegetation proportions and Digital Numbers from the NDVI of the study area (Aravind et al., 2022).

$$E = 0.004 * PV + 0.986 \quad Eq. 4$$

PV is the NDVI proportion (relation between $NDVI_{min}$ and $NDVI_{max}$)

0.986 is the correction value

Land surface temperature (LST)

Land Surface Temperature (LST), representing the radiative skin temperature, is derived by considering the wavelength of emitted radiation, the brightness temperatures at the top of the atmosphere, and the land surface emissivity (Aravind et al., 2022).

$$LST = BT / (1 + (\lambda * BT / C_2) * \ln(E))$$

Eq. 5

In this equation, BT is the Brightness temperature, λ is the emitted radiance wavelength, E is the Land surface emissivity, and C_2 is a constant (14388 mk)

By following the above steps, the LST data from the Landsat satellite image can be estimated.

Urban Heat Island Intensity Index

Urban heat island intensity index is usually measured by how much warmer cities are compared to its peripheral non-urban areas (Martin-Vide et al., 2015). By using land use maps to find the average surface temperature for each land type, the urban heat island level can be determined by comparing it with the temperature in cities to the temperature of their surroundings (Rendana et al., 2023). The average surface temperature for each land use category can be determined by relating it to the land use map, which allows us to represent urban heat island intensity by the LST changes between urban and surrounding areas (Rendana et al., 2023). For this study, the rural areas are not given a separate land class. The underdeveloped pristine areas in the vicinity of the study area are being used as the reference (mountain range) for the UHII calculations. The UHI intensity index is split into five classes, from very low to very high (Table 3).

$$UHI = (Ti - Ts) / Ts$$

Eq. 6

Here, the T_i denotes the mean LST of each land use class, and T_s represents the mean LST of rural areas, which in this case is mountain ranges.

UHI index range	Class	Discription
< -0.152	Very low	Areas that have very low temperatures (no variation in T_i and T_s)
-0.152 to 0.005	Low	Low temperature with little variance in T_i and T_s
0.005 to 0.16	Medium	Moderate temperature (moderate variations)
0.16 to 0.32	High	High temperatures with significant variations
0.32 >	Very high	Very high temperatures (high T_i and T_s variations), also considered as hot spots.

Table 3: UHI Intensity Ranges

LULC, LST, and UHI prediction

For the prediction of the land dynamics, the MOLUSCE plugin from the QGIS software was used. The MOLUSCE plugin uses a CA-ANN model which helps to forecast LULC, LST, and UHI, it was created by the ASS (Asia Air Survey) for the QGIS software (Kulithalai Shiyam Sundar & Deka, 2022). The model helps us to effectively forecast or predict the land cover changes and also provides valuable information to make decisions about future developments (Mishra et al., 2024). The CA-ANN model in the MOLUSCE forecasts spatial land use and land cover transitions by assessing a pixel's present value in relation to its initial condition, neighbouring influences, and established changeover rules (Mishra et al., 2024). The LULC changes are first identified by the model then the future changes are predicted (Aneesha Satya et al., 2020).

The changes that are observed in the LULC are seen by inspecting the changes in pixel value (Abbas, Z et al., 2021). The MOLUSCE is an integration of ANN and CA linked by geographical networks (X. Liu et al., 2017). ANN model is able to deal with large and complex data, making it suitable for this study (Gantumur et al., 2022). The 2020 and 2024 data is used as the initial and final layers in the model. Similarly, the independent variables are also added in order to get a realistic prediction. Before using the data, the map layers are ensured to have the same geometries to avoid any errors.

In the phase of modelling the ANN will calculate the probability of the grid cell, exchanging into different LULC classes (Xiang et al., 2024). The cellular automata model can simulate the spatial patterns of land use and land cover (LULC) and the UHI intensity based on defined transition rules, and then create maps illustrating the distributions (Xiang et al., 2024). The LST and UHI intensity data are reclassified into five classes and follow the same method as for LULC prediction. Instead of the spatial variables used for LULC, other parameters like NDVI (Normalised Difference Vegetation Index), NDBI (Normalised Difference Built-up Index), and NDWI (Normalised Difference Water Index) are used for the forecasting of LST and UHI intensity.

6. RESULTS

The LULC classification was accomplished using Machine learning through a Random Forest model. The accuracy assessment was also done to check whether the classification was reliable. In terms of the accuracy assessment, the overall accuracy and kappa coefficient were 88% and 0.91 for 2016, 90% and 0.87 for 2020, and 83% and 0.81 for 2024, as illustrated in Table 4. The LULC dynamics between 2016 and 2032 suggest changes between different land covers, like barren land, fallow land, vegetation, built-up, water bodies, and forest-mountain ranges.

Time	Overall accuracy	Kappa coefficient
2016	88%	0.91
2020	90%	0.87
2024	83%	0.81

Table 4: Overall accuracy and Kappa coefficient

LULC status of 2016

In 2016, barren lands occupied more areas than the other classes. It covers about 418.91 sq. km (35%) of the total land. The Fallow land occupies 262.75 (21.95%). Both the barren land and fallow land covered 56% of the total study area, suggesting a large area that is left undeveloped and unused. The vegetation accounted for 201.98 sq km (16.87%), and the built-up areas constituted 171.14 sq km (14.3%). The water bodies only cover an area of 5.18 sq. km, and the forest-mountain areas contribute 137.08 sq. km (11.45%). (Fig. 3)

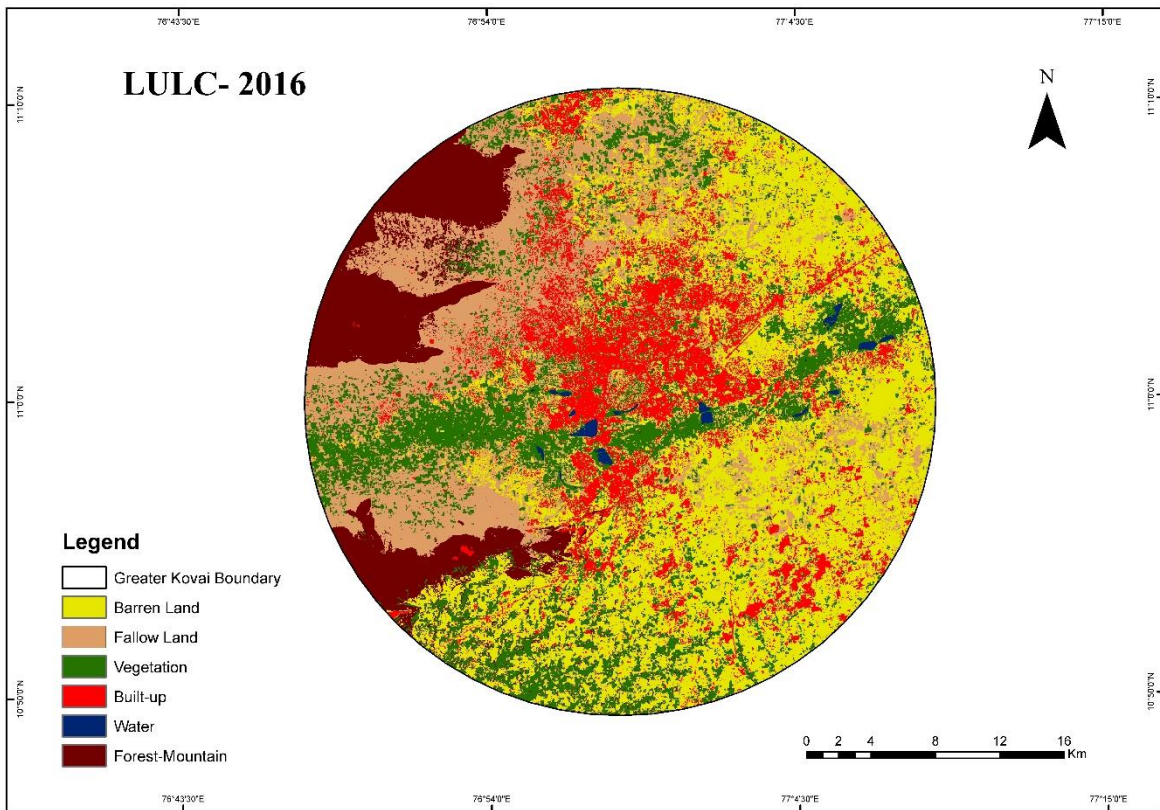


Fig. 3: LULC of 2016

LULC status of 2020

Some major changes were observed in 2020; the barren land has decreased to 338 sq. km (28.24%), which may be converted to fallow or vegetation. The fallow land increased significantly to 417.4 sq. km (34.87%), which may be due to the abandonment of agricultural practices or shifting cultivation patterns. The vegetation cover decreased to 145.8 sq. km (12.18%), indicating deforestation or land degradation. The built-up areas were found to have decreased during this time by 159.67 sq. km (13.34%). The water and mountain ranges were found to be stable at 0.66 and 10.71 %, respectively. (Fig.4)

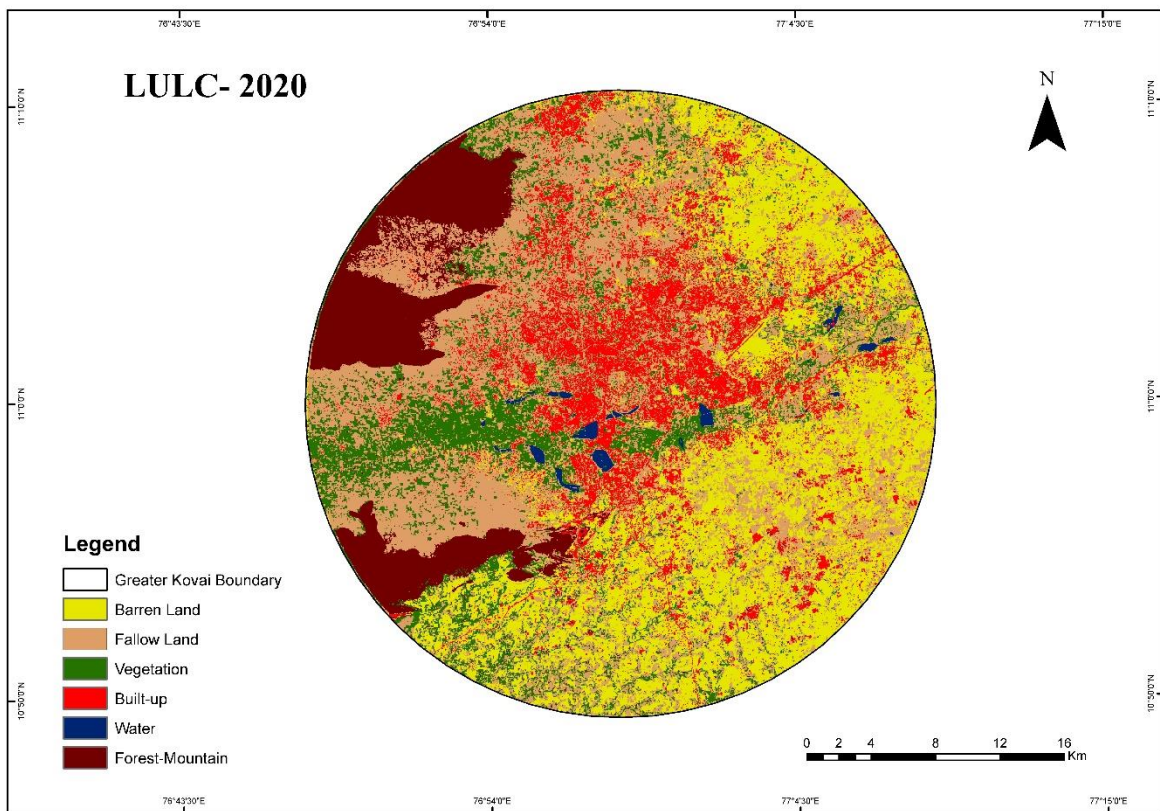


Fig. 4: LULC of 2020

LULC status of 2024

In 2024, the barren lands again increased to 368.3 sq. km (30.86%), which may be due to land left idle after cultivation. Fallow land decreased slightly to 306.53 sq. km (25.68%). The vegetation recovered to 194.54 sq. km (16.3%), indicating efforts for reforestation and sustainable land use. Built-up increased to 173.57 sq. km (14.54%), water bodies and mountains remained steady with both 0.61% and 12% respectively. (Fig.5)

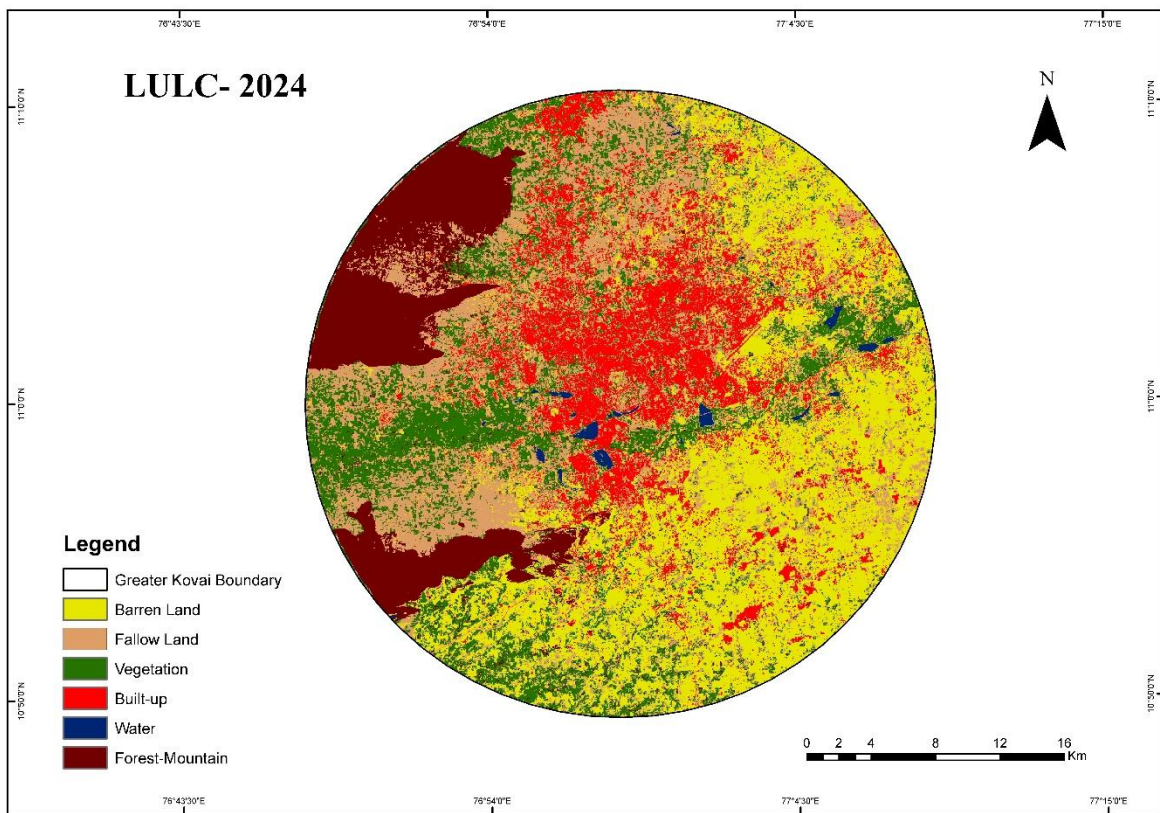


Fig. 5: LULC of 2024

LULC projections for 2028 and 2032

The future projections indicated a steady rise in built-up areas, rising to 194.67 sq. km (16.31%) by 2028 and 210 sq. km (17.6 %) by 2032. The barren and fallow lands projected a steady decrease by 2028 and 2032, 355.18 sq. km (29.76%), 302.35 sq. km (25.33%) and 340 sq. km (28.49%), and 300 sq. km (25.14%), respectively. The vegetation remained stable at 197.81 sq. km (16.57%) in 2028 and experienced a decline in 2032, to 192 sq km (16.09%). The water bodies dropped back to 5.2 sq. km (0.44%) in 2028 (Fig.6) and remained the same in 2032 (Fig.7). The mountains remained the same throughout 2028 and 2032, at 11.6 %.

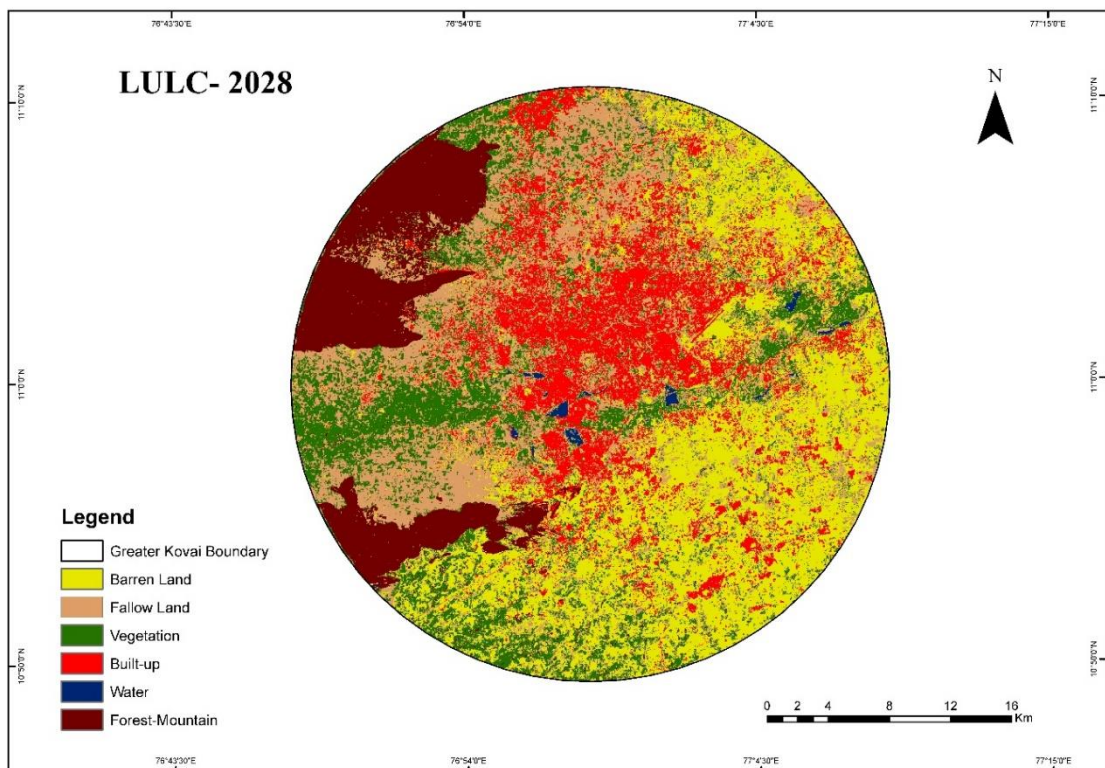


Fig. 6: LULC of 2028

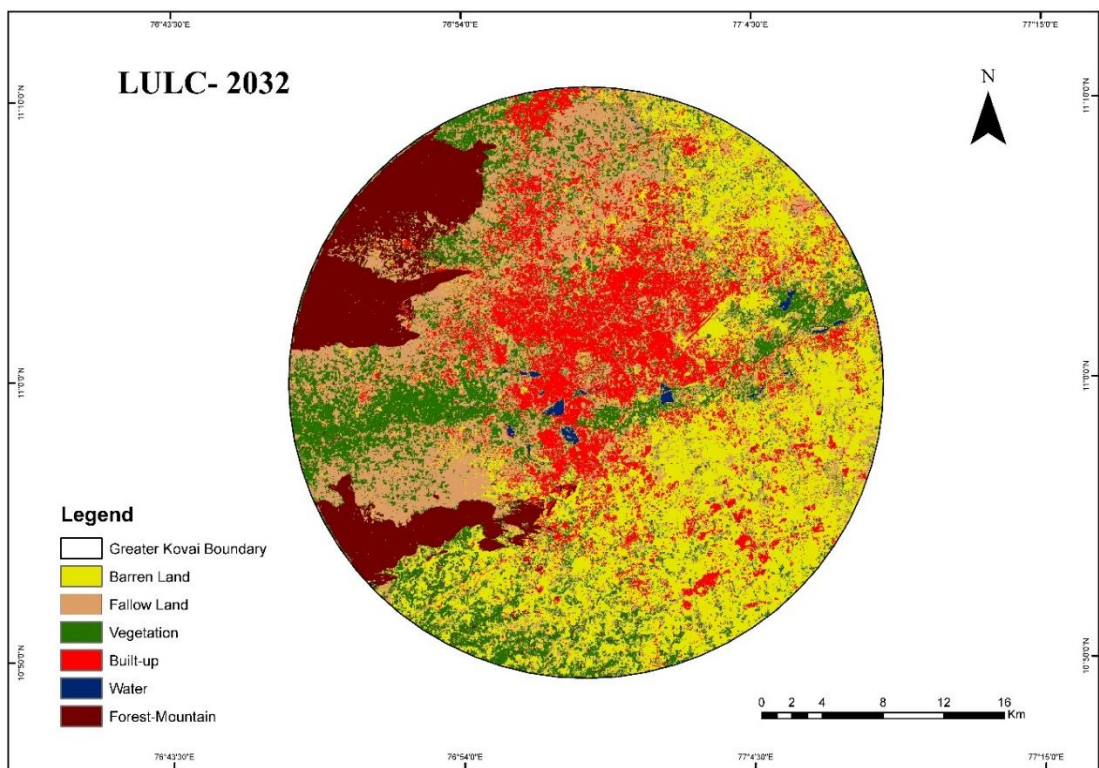


Fig. 7: LULC of 2032

Temporal LULC changes (2016-2032)

The study area experienced a gradual increase in built-up area from 14.3% in 2016 to 17.6% in 2032, reflecting ongoing urban expansion. Barren land showed a steady decrease from 35% to 28.49%, suggesting that some of the unused land was transformed into other uses. Fallow land increased from 21.95% to 25.14%, indicating a possible shift in agricultural practices. Vegetation slightly declined from 16.87% present to 16% (Table 5), pointing to a minor green cover loss. Water bodies remained almost the same, as well as the mountain areas. (Fig. 8)

Class	2016 (km²)	2020 (km²)	2024 (km²)	2028 (km²)	2032 (km²)	2016 (%)	2020 (%)	2024 (%)	2028 (%)	2032 (%)
Barren	418.91	338	368.35	355.18	340	35	28.24	30.86	29.76	28.49
Fallow	262.75	417.4	306.53	302.35	300	21.95	34.87	25.68	25.33	25.14
Vegetation	201.98	145.8	194.54	197.81	192	16.87	12.18	16.3	16.57	16.09
Built-up	171.14	159.67	173.57	194.67	210	14.3	13.34	14.54	16.31	17.6
Water	5.18	7.94	7.28	5.2	5.2	0.43	0.66	0.61	0.44	0.44
Forest- Mountains	137.08	128.24	143.25	138.45	138.45	11.45	10.71	12	11.6	11.6

Table 5: Area and Percentage of LULC

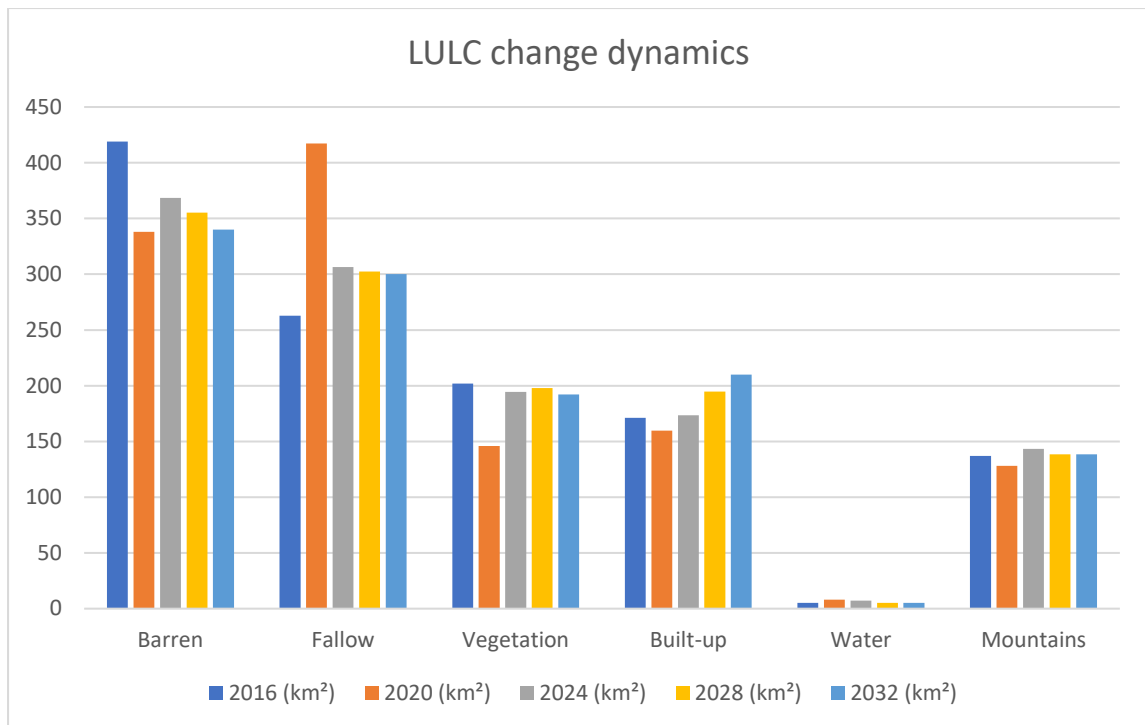


Fig. 8: Graphical representation of LULC change dynamics

LST Distribution

The LST extraction was done using the ArcMap software, in which a step-by-step process was followed. It is generally done by calculating the TOA, BT, NDVI, emissivity, and then the LST. After the calculation, the LST is reclassified into five distinctive classes from very low to very high. (Table 6)

Temperature	Class
<25°C	Very low
25-30°C	Low
30-35°C	Moderate
35-40°C	High
>40°C	Very high

Table 6: LST Class ranges

LST Distribution

In 2016, the area under 35 °C to 40 °C was the highest at 765.44 sq. km (Fig. 9), with approximately 157 sq. km experiencing temperatures above 40 °C. Around 255 sq. km fell within the 30 °C to 35 °C category. By 2020, there was a notable decrease in temperature. The

area under $<25^{\circ}\text{C}$ saw a sharp increase to 7.74 sq. km (Fig. 10), and the area between 25°C and 30°C rose to 80 sq. km. The area under 35°C to 40°C decreased to 603 sq. km. In 2024, the area under $<25^{\circ}\text{C}$ sharply fell to 0.14 sq. km, 25°C to 30°C decreased to 38.43 sq. km, while the area above 40°C increased to 195.87 sq. km. (Fig.11) There was notable cooling in 2020, but temperatures rose again in 2024, continuing a warming trend. Despite the temporary cooling in 2020, 2024 experienced a return to heat stress conditions in high-temperature zones.

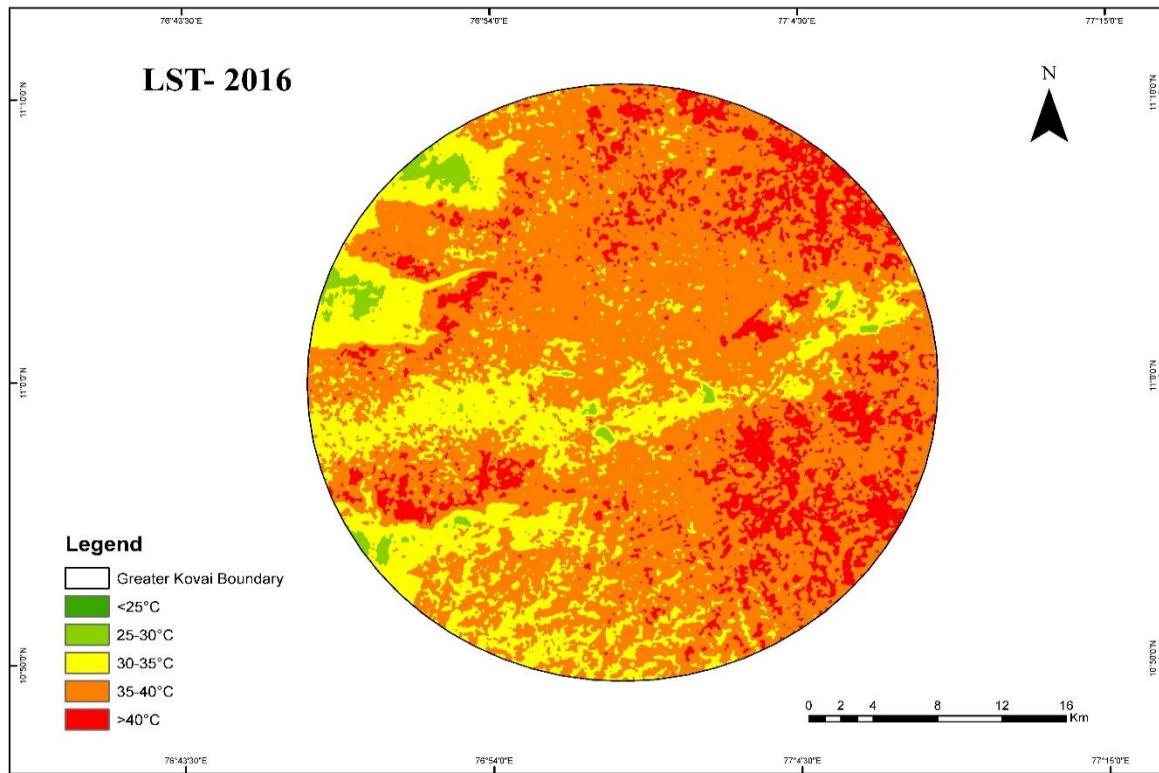


Fig. 9: LST of 2016

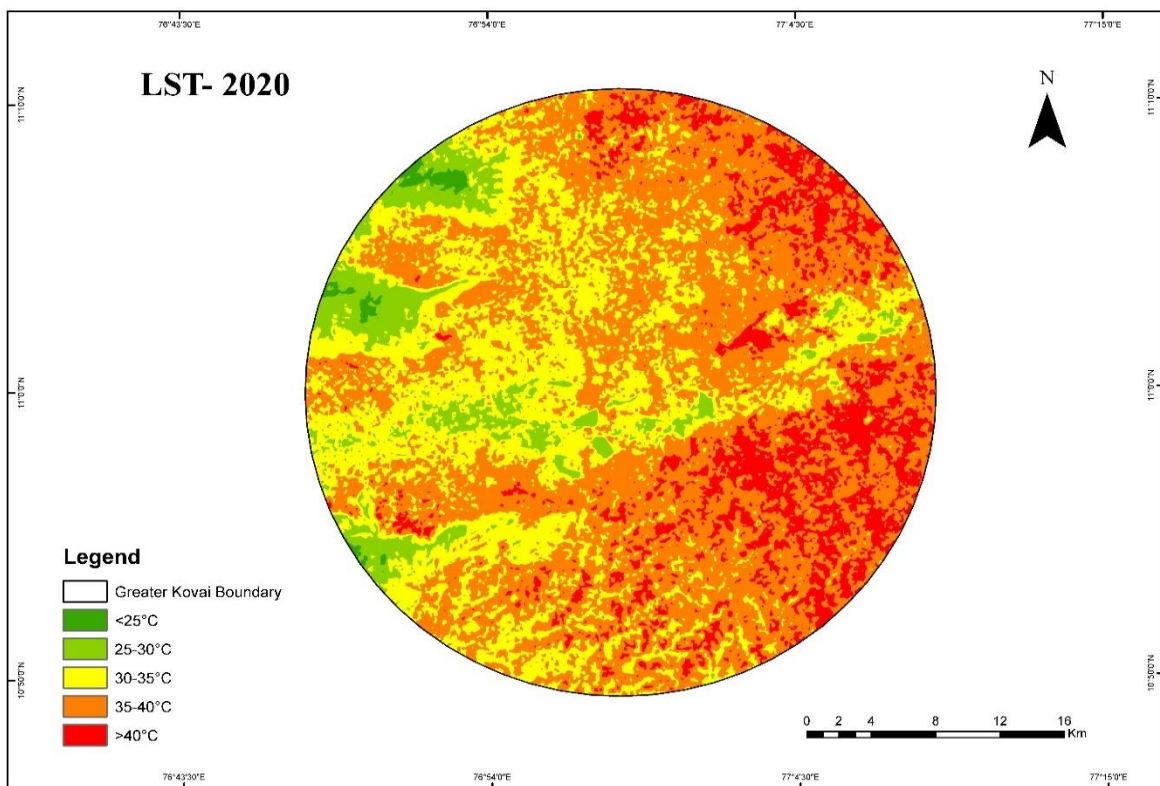


Fig. 10: LST of 2020

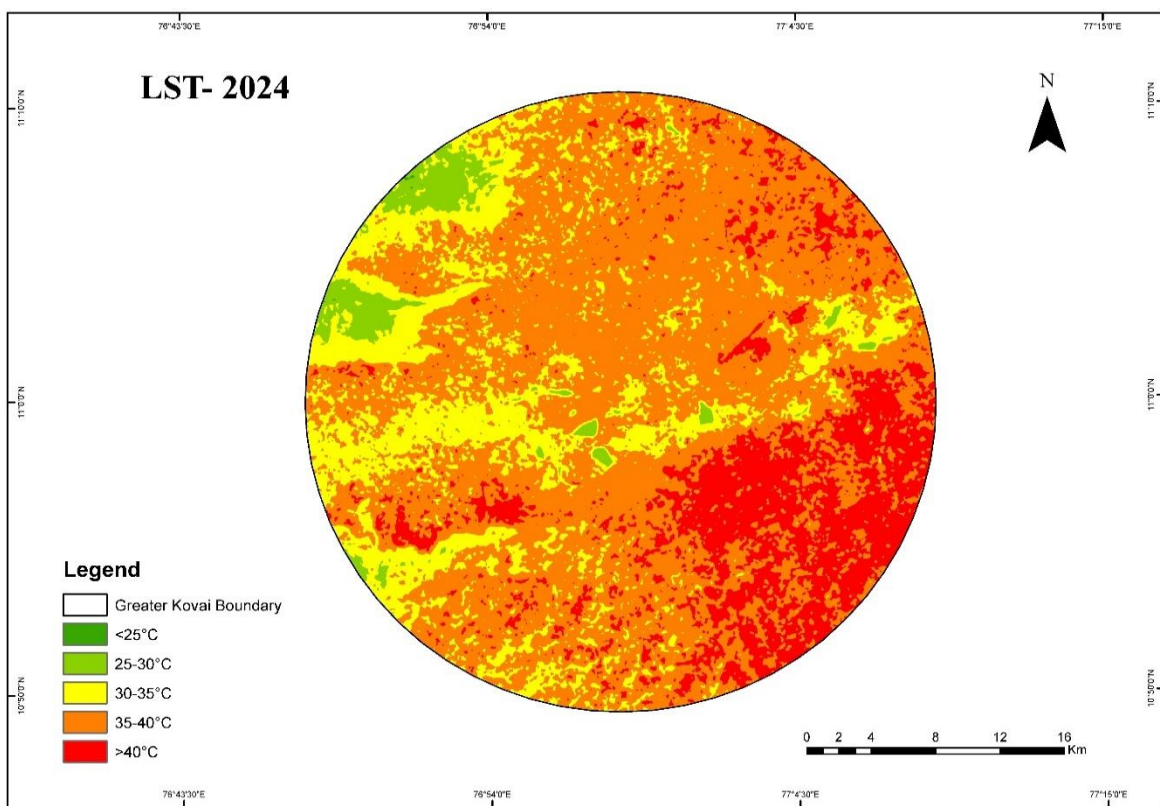


Fig. 11: LST of 2024

LST Projection for 2028 and 2032

In the projected 2028, the above-40 °C zone increased to 237.01 sq. km, and the 35- 40 °C zone remained high at 709 sq. km (Fig. 12). The areas in the cooler zone (25-35 °C) remained the same. By 2032, the trend remained the same. Some minor changes are seen in the higher temperature zones. The above-40 °C zone slightly decreased to 235 sq. km, and the 35- 40 °C zone increased to 715 sq. km (Fig. 13).

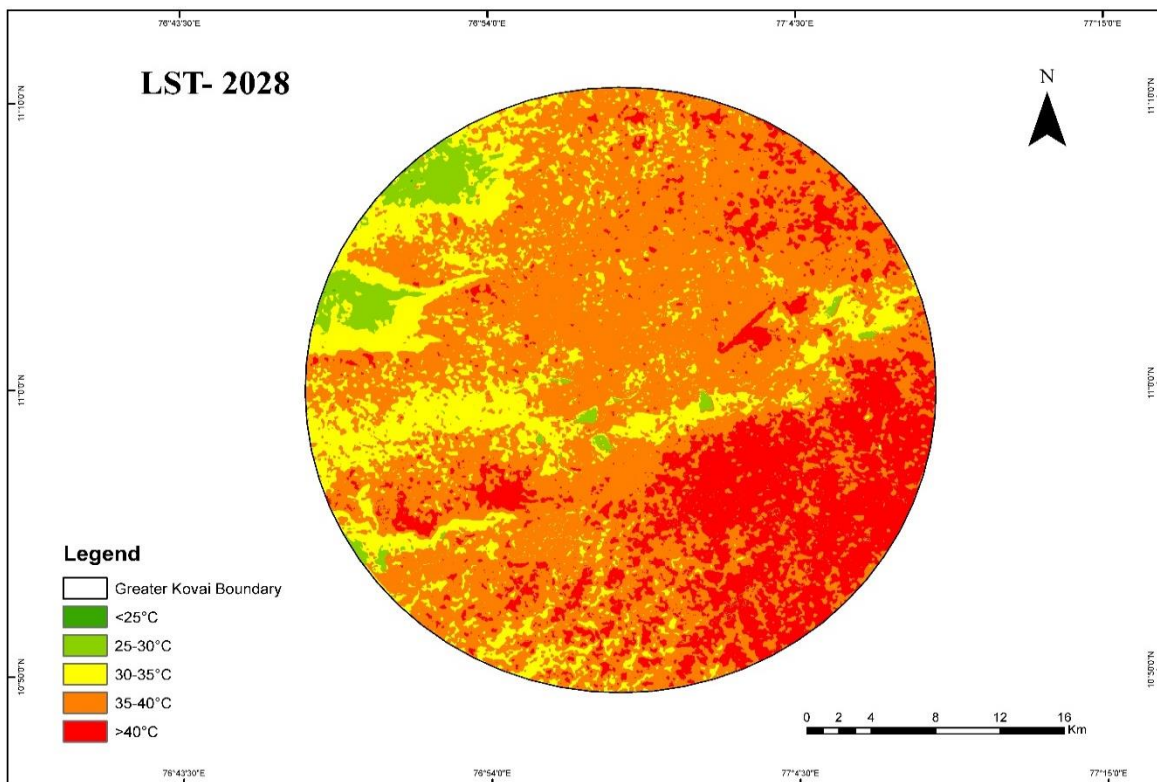


Fig. 12: Predicted LST of 2028

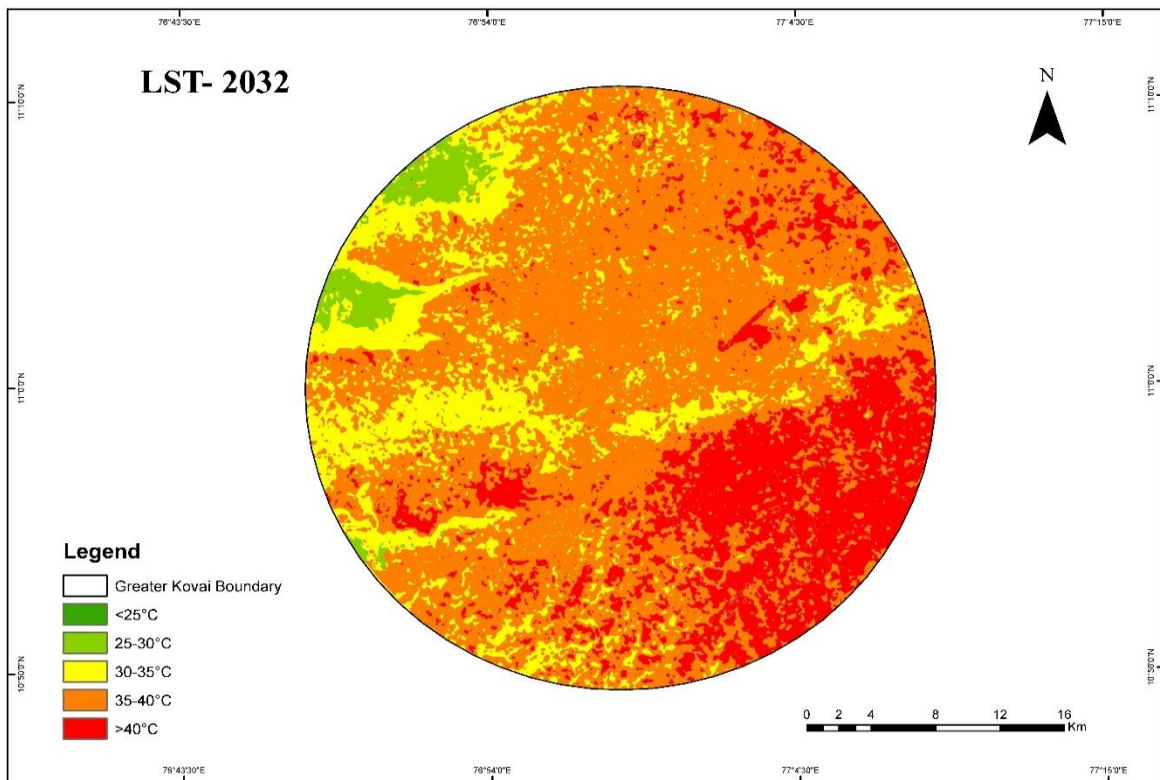


Fig. 13: Predicted LST of 2032

Both projected years have continued to experience warming trends, with the 35-40 °C (Table 7) zone occupying the most area. The above 40 °C zone also showed a steady increase, indicating heat stress mainly due to increased settlements and loss of green area (Fig. 14)

Year	<25°C	25-30°C	30-35°C	35-40°C	>40°C
2016	0.0153	19.8432	255.2994	765.4383	156.465
2020	7.74	80.0757	359.3538	603.1683	146.7162
2024	0.1431	38.43	239.6142	722.1708	195.8697
2028	0.0828	37.5696	212.4999	709.0632	237.0123
2032	0.0828	33.444	211.4163	715.392	235.8927

Table 7: LST area zones

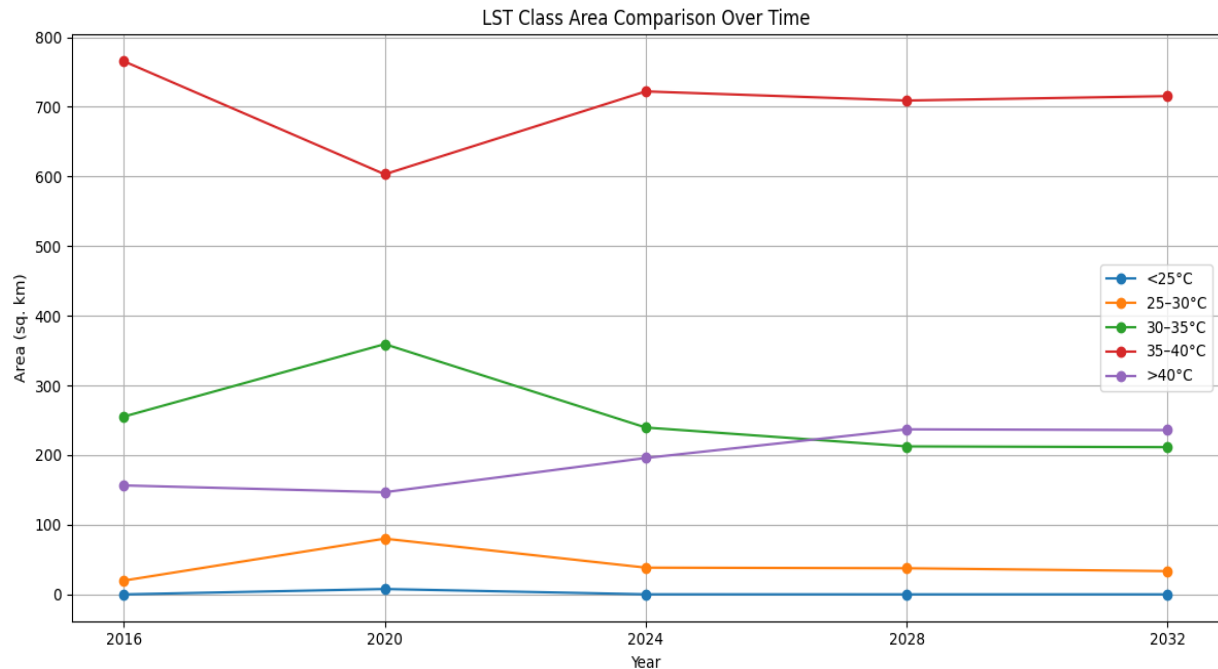


Fig. 14: LST Class Area Comparison over Time

UHI Intensity trend analysis

The results examine the trends in Urban Heat Island (UHI) intensity across distinct periods, indicating the shifts in the distribution of heat and the implications it imposes.

2016-2024: Transition Phase

In this phase, a small reduction was observed in the ‘very high’ zones. The UHI intensity was observed to decrease from 296.97 sq. km in 2016 (Fig.15) to 201.41 sq. km in 2024 (Fig. 17). The “Moderate zones” indicated an increase in area from 315.28 sq. km to 400.07 sq. km. This shift suggests a change in the distribution of heat from very high zones to moderate zones. Minor changes are seen in the “Very low” and “Low” zones, as they were stable throughout the study period. The results from 2016 to 2024. There has been a reduction in heat zones during the period of 2016-2014, this may be due to short-term improvements like increased vegetation cover or land use changes. This period also indicated a persistence in heat stress, in a more widespread form, therefore showing that there is no complete reduction in heat stress.

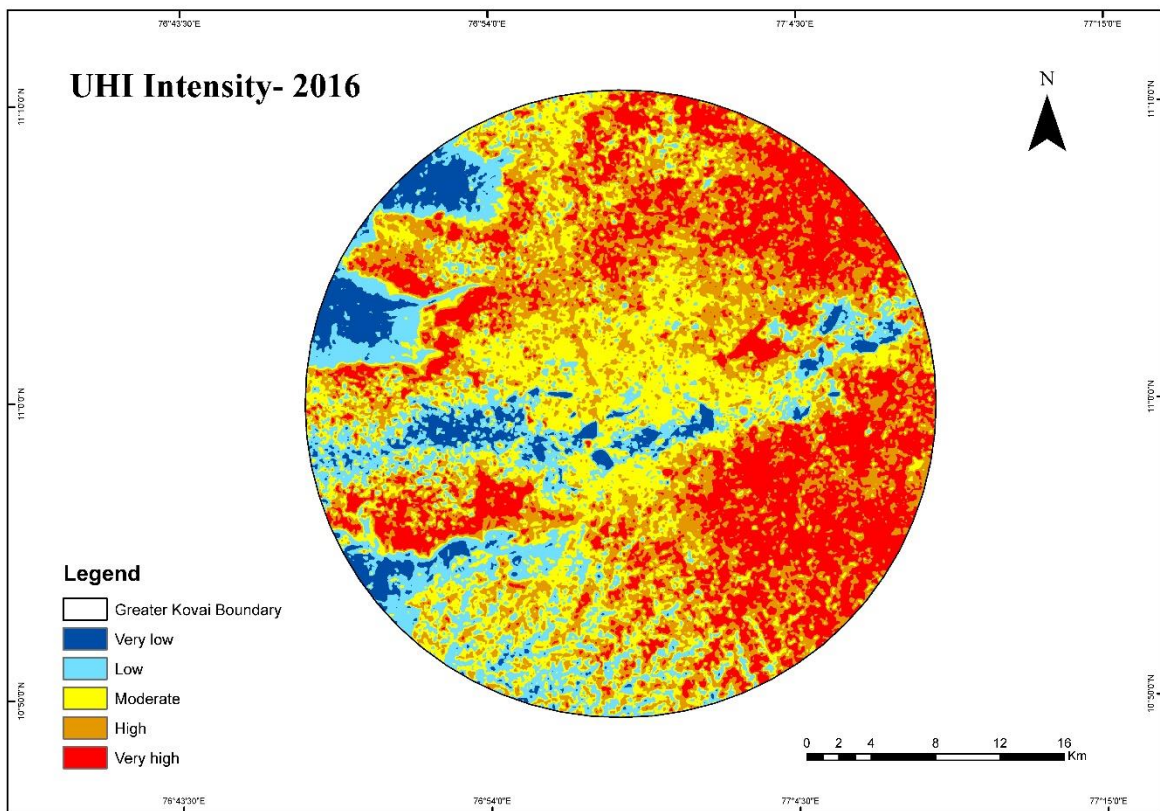


Fig. 15: UHI intensity of 2016

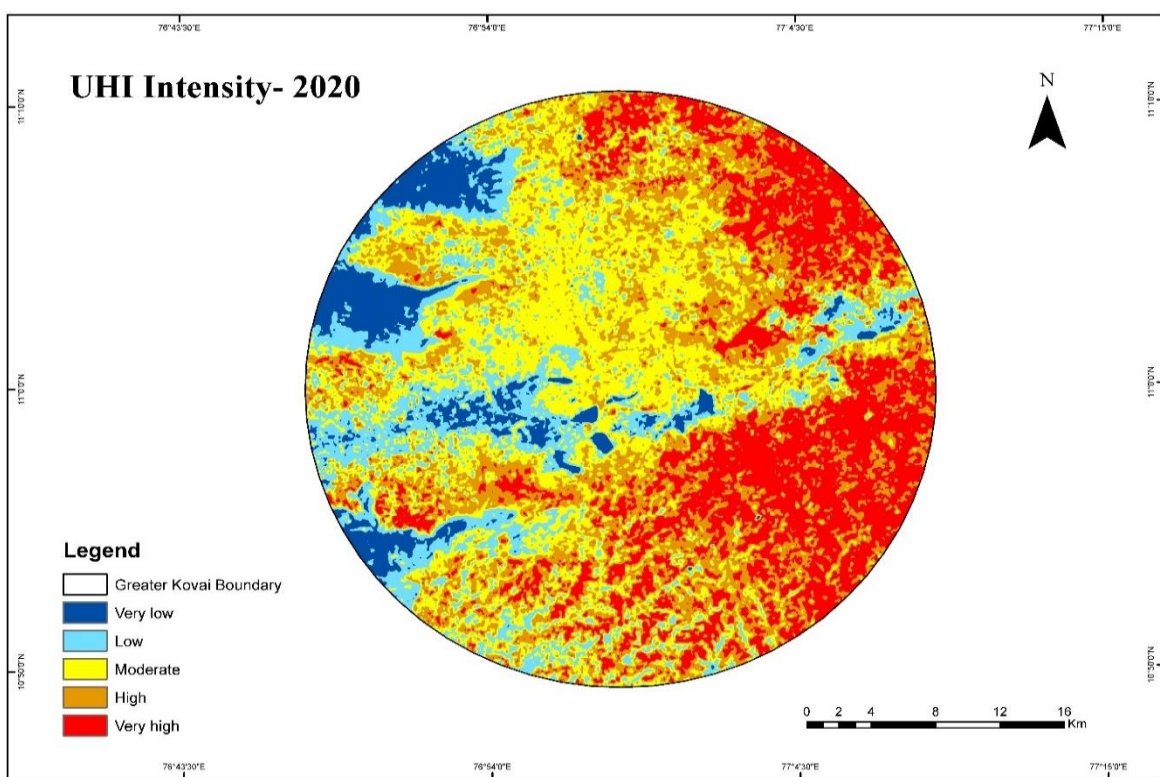


Fig. 16: UHI Intensity of 2020

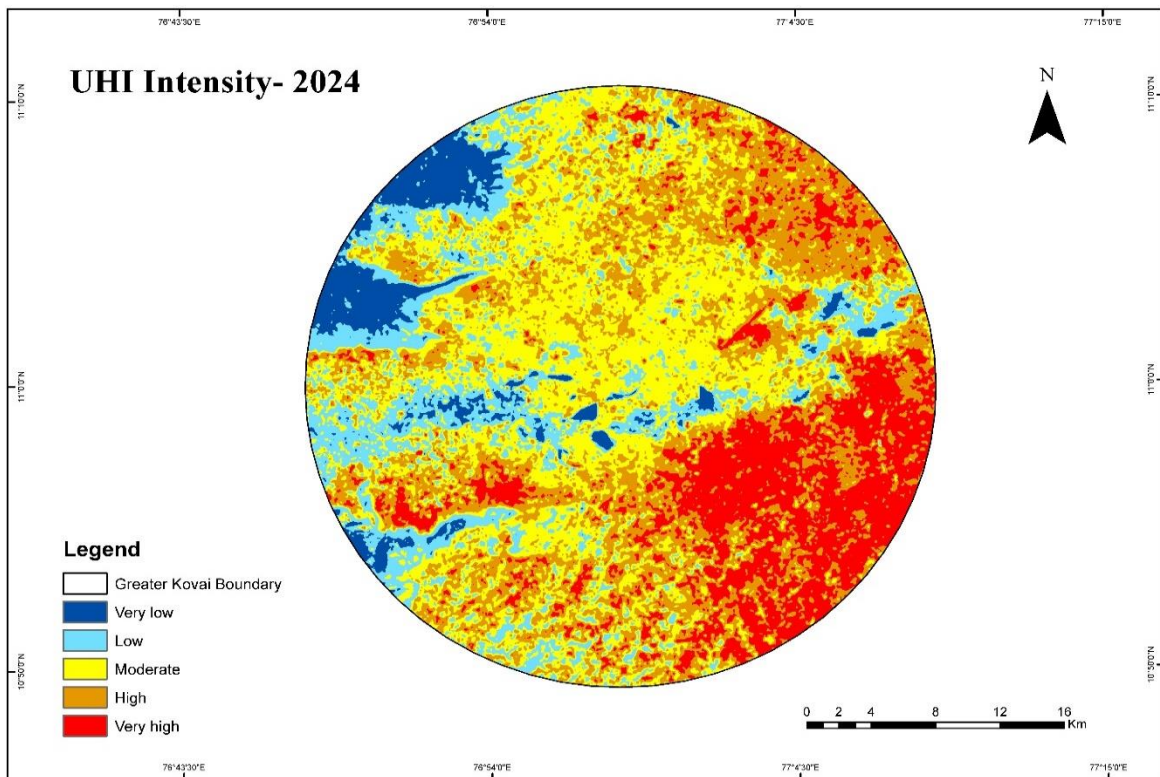


Fig. 17: UHI Intensity of 2024

2028- 2032: UHI intensity projection

In the projected 2028 and 2032 UHI intensity, the warming is again reinforced. In the period from 2028 to 2032, there has been an increase in the “High” zones, reaching an area of 387.44 sq km by 2032 (Fig. 19), reaching its highest across the years. Subsequently, there has been a slight decrease in the “Very High” zones, reaching an area of 168.99 sq. km. this indicates that although there has been a decrease in the very high zones, there has been an increase in the high zones; it does not fully reduce the effect of heat stress, but redistributed in other areas. The “moderate” zone remained constant at approximately 374.8 sq. km, also the “very low” and ‘low’ zones experienced no changes indicating that there is no significant cooling seen in the areas (Table 8). The trends seen from 2028, (Fig. 18) stipulate that although there has been a decrease in the “very high” zones, there is also no changes seen in the “very low” and “low” indicating no cooling trend. The UHI intensity have observed to re-distribute and accumulate in the “high” zones. This may be due to the changes in Urban expansion. Such conditions can lead to harmful effects such as thermal discomfort and widespread distribution of heat stress across the area, even though there is a steady decrease in “very high” zones.

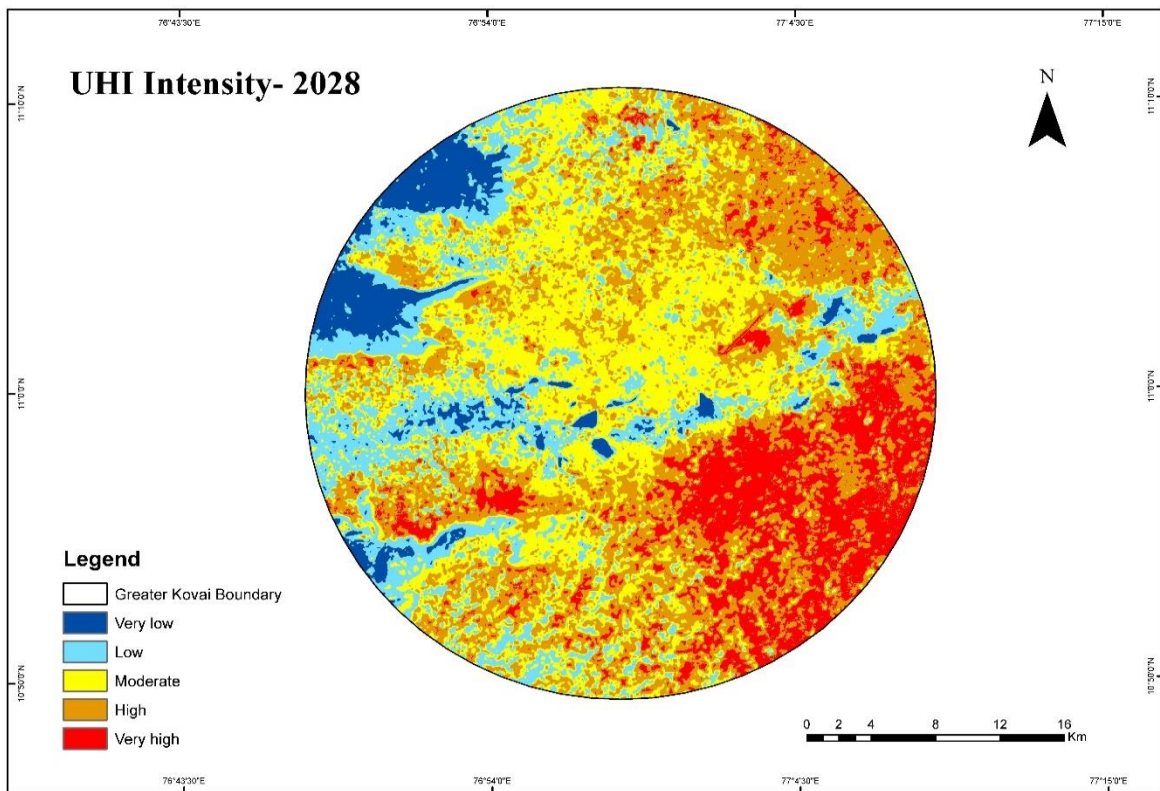


Fig. 18: Predicted UHI Intensity of 2028

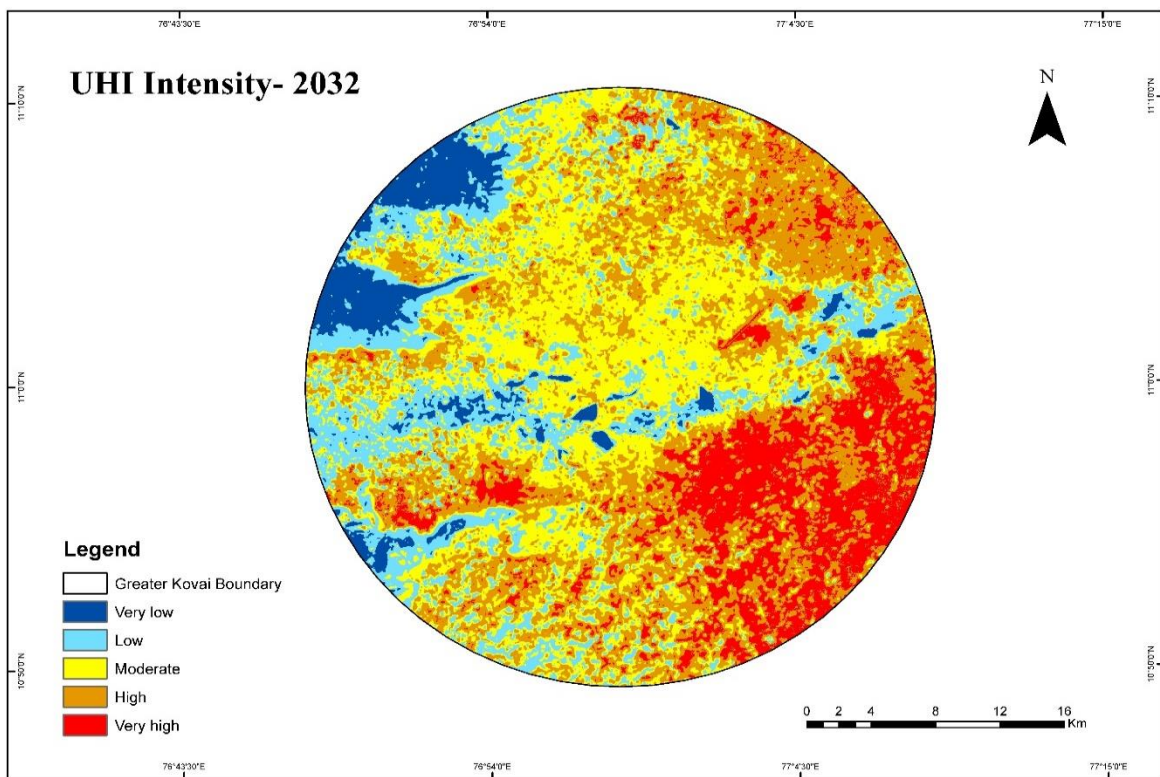


Fig. 19: Predicted UHI Intensity of 2032

Year	Very Low (Sq. km)	Low (Sq. km)	Moderate (Sq. km)	High (Sq. km)	Very High (Sq. km)
2016	67.1022	176.0184	315.2844	341.6886	296.9676
2020	78.0759	171.8523	354.2301	329.544	263.3517
2024	67.5414	172.9881	400.0716	354.2166	201.4101
2028	67.4469	197.6058	374.8059	386.8191	169.5501
2032	67.437	197.55	374.8014	387.4401	168.9993

Table 8: UHI Intensity Area Zones

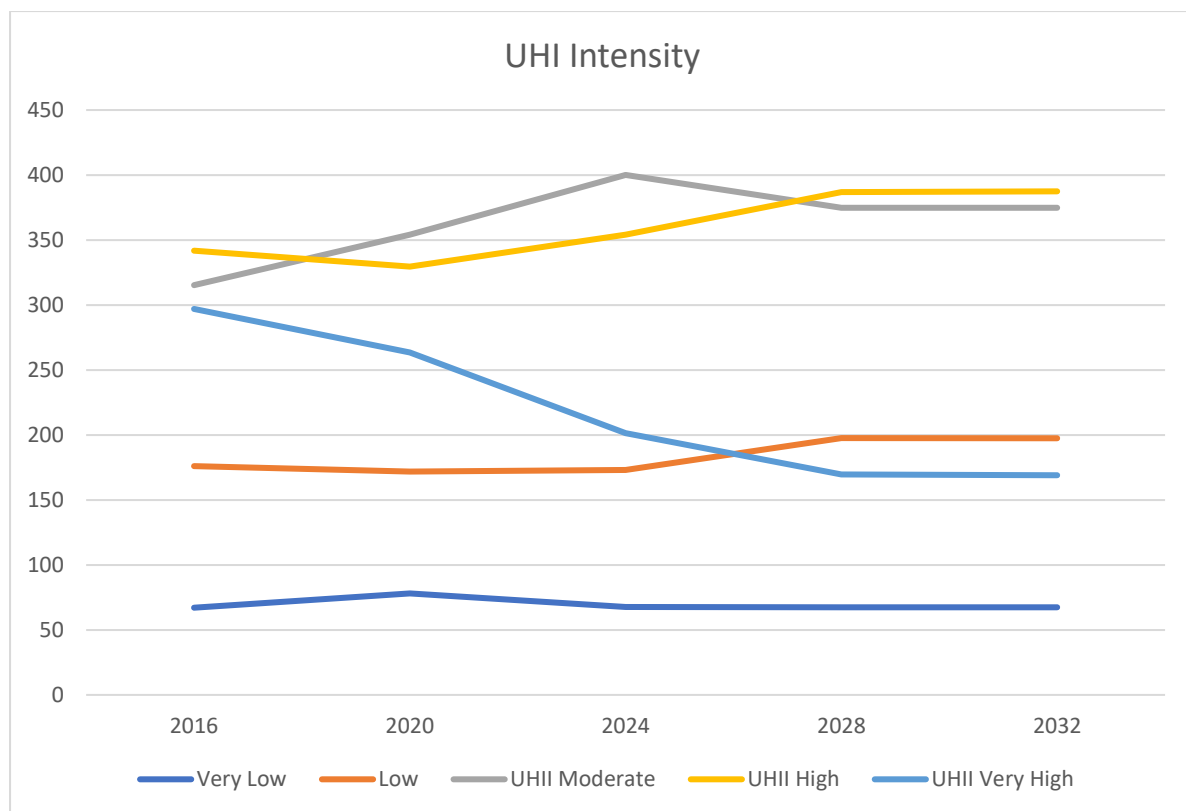


Fig. 20: UHI Intensity Comparison Graph

7. DISCUSSION

Over the years, there have been some notable changes in the LULC. In 2016, the barren land occupied the most area with 35%, followed by fallow land with 21.95%. The vegetation accounted for about 17%, and the built-up area with around 14% (Fig. 21). The Forest-Mountain cover comprises 11.45 % of the total land cover, while the water bodies only account for 0.43 %. By 2032, some notable changes were seen. The barren land still occupied the majority of the area, but decreased to 28.5% (Fig. 22). The Fallow land experienced an increase of 3.19 %, accounting for 25.14 %. The vegetation class remained more or less the same, with 16.09 %, indicating strong conservation efforts. There has been a steady increase in built-up in the study period throughout the years. By 2032, the built-up area will have reached its maximum with 17.6%, an increase of 3.3% from 2016. The water bodies and Mountain ranges remained the same with 0.44% and 11.6 %, indicating no changes in the topography.

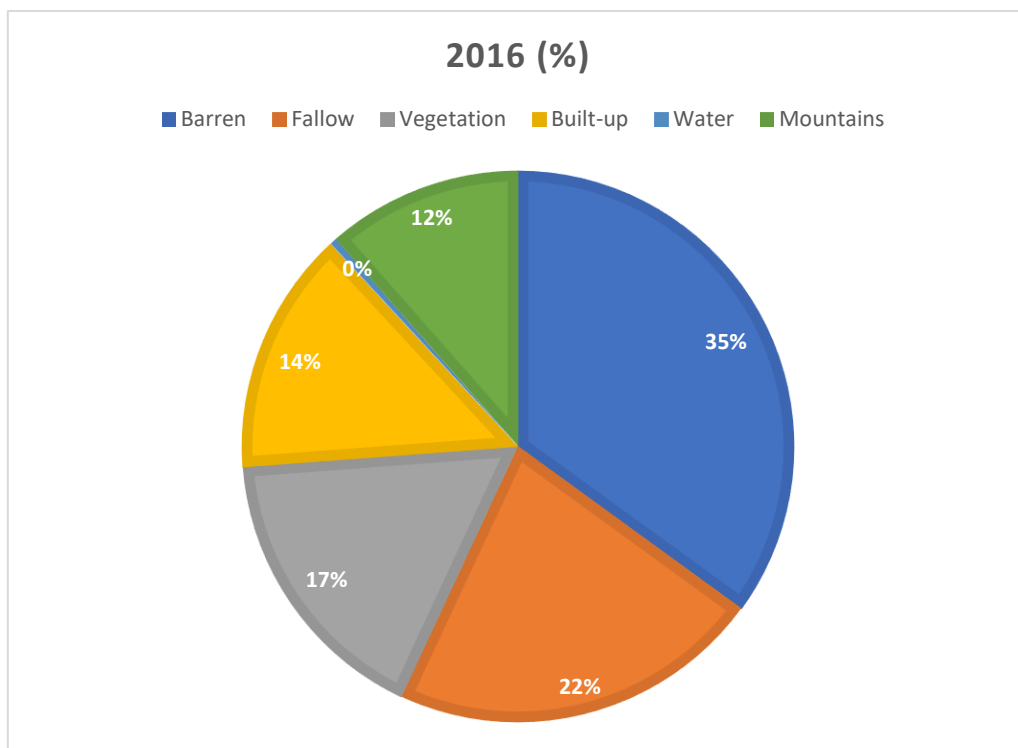


Fig. 21: Total percentage area of each LULC class in 2016

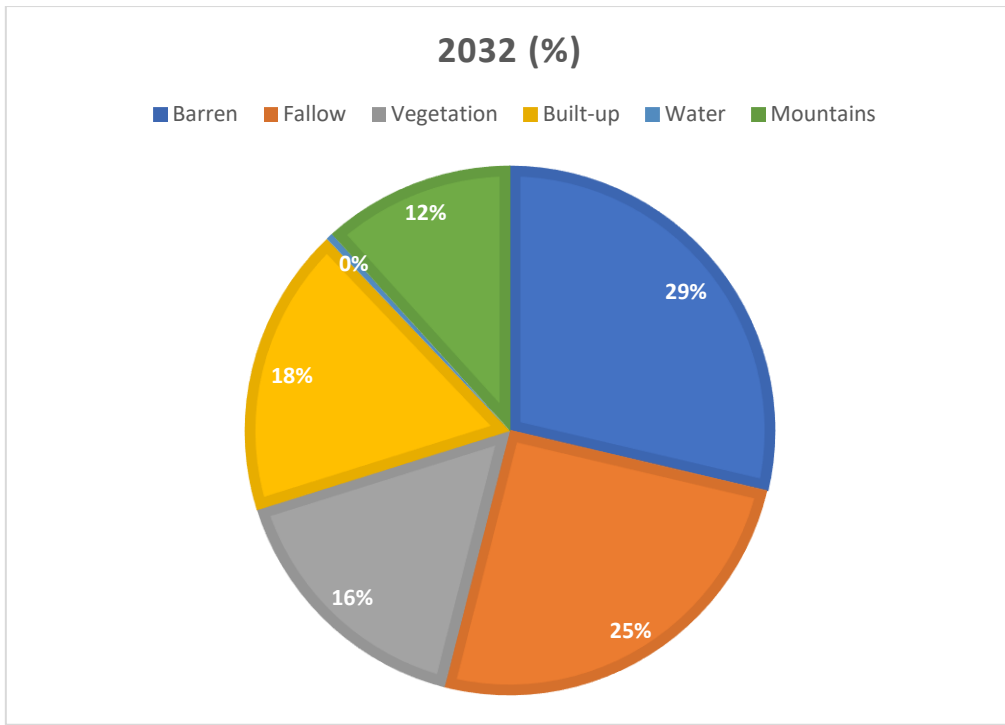


Fig. 22: Total percentage area of each LULC class in 2032

There has also been a steady increasing shift in the LST across the study area. Although the average LST remained the same, there has been an increase in the areas undergoing high temperatures. To verify the LST data, it was compared with the near surface air temperature in the nearby weather station, in this case, the Coimbatore International Airport (Table 9). This method is widely used for verifying the reliability of LST.

Time	Air temperature	Surface temperature
2016-03-20	33°C	36°C
2020-03-31	32°C	35°C
2024-03-26	32°C	36°C

Table 9: Comparison of Air and Surface Temperature

The LST data reveals that the barren land has the highest average temperature compared to other land cover, 35°C in 2016, 38°C in 2020, and 36°C in 2024 (Table 10). It was also observed that the fallow land and the Built-up had similar average temperatures in 2016, 2020, and 2024.

In hot, arid environments, increasing vegetation and swimming pools help lower the land surface temperature (LST) through evapotranspiration, while expanding bare soil has the opposite effect due to fast radiation of solar energy (Li, X., et al., 2016). This may be the possible reason for the similarity in average LST in the Fallow land and the Built-up area. The water bodies had the lowest mean temperature with 27°C in 2016, 2020, and 2024.

Class	2016 (°C)	2020 (°C)	2024 (°C)
Barren	35.71584	38.90741	36.65343
Fallow	35.35862	36.12549	34.31612
Vegetation	31.48697	32.7968	31.76848
Built-up	34.31072	36.16359	34.11464
Water	27.22211	27.78414	27.21099
Forest- Mountain	30.3639	30.47887	29.59594

Table 10: Average LST of each Land Class

For a clear understanding of the gradual increase of LST, it is classified into two distinctive classes, area under the <35°C and >35°C. the graph shows that there is an increasing shift in the >35°C (Fig. 23) and a decreasing shift in the <35°C (Fig. 24).

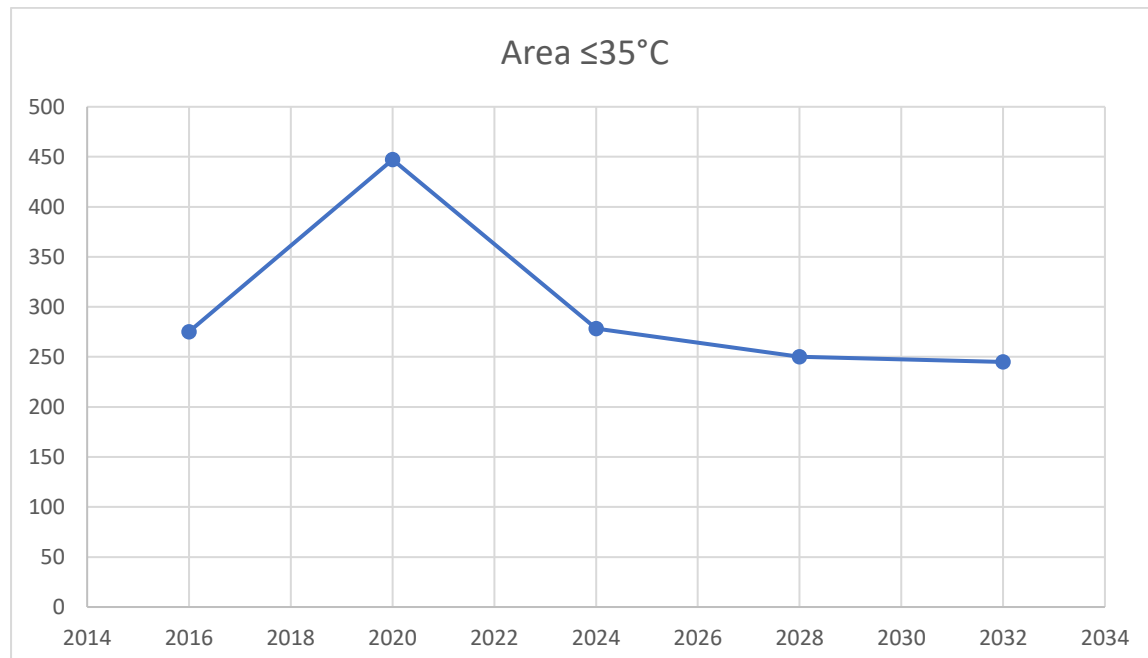


Fig. 23: Area under <35°C

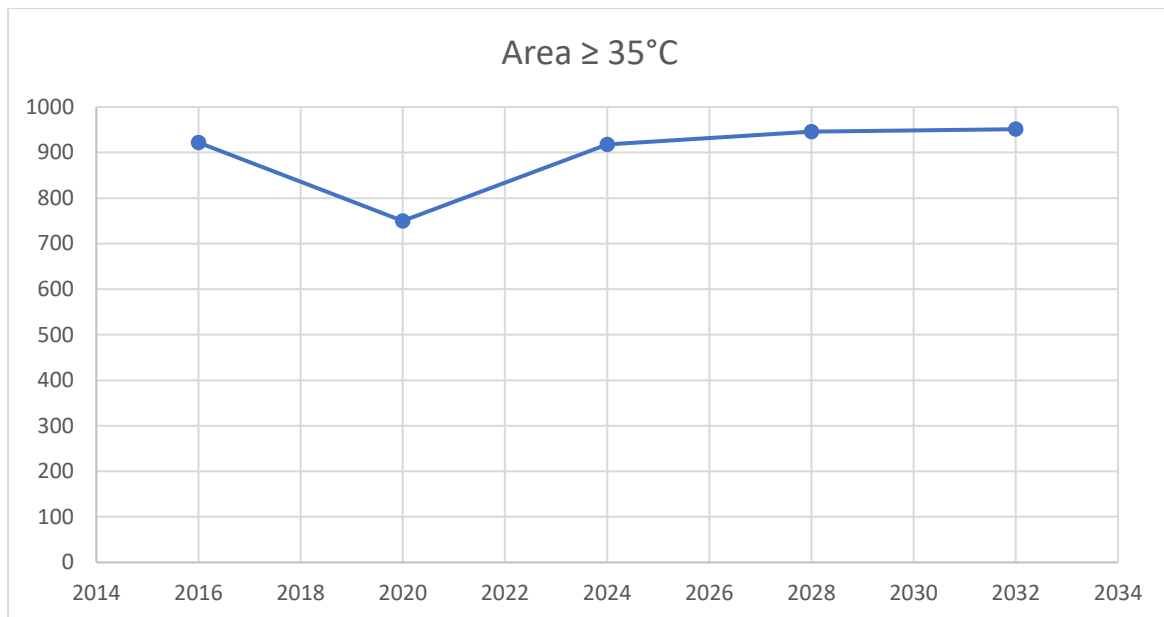


Fig. 24: Area under $>35^{\circ}\text{C}$

There have been some changes observed in the Urban heat island Intensity across the study area. Although there were notable changes from 2016 to 2024, the model predicted a stable state during 2028 and 2032. The data discovered that there has been a significant decrease in area coming under the “Very high” zones from 2016 to 2032, however, there has been an increase in area under the “Moderate” and the “High” zones. This shows that there is a more widespread heat across the area, signalling the redistribution of heat stress. The stabilising nature of UHI intensity even through the increase in LST is discussed in a study by (Zhou et al., 2014) explaining that there were some changes seen in the Surface UHI intensity over an area which can only be explained by surface heating alone, during the daytime in summer. The study also indicated that the effect of surface mechanisms and climate does not have a significant role in UHI intensity, hence, the gradual increase in LST does not affect UHI intensity. Similarly, (Peng et al., 2018) found that urban land surface temperature increased more slowly during the day but faster at night compared to rural areas, suggesting that the difference in temperature between urban and rural areas tends to reduce at sunlight and elevate at night.

8. CONCLUSION

The LULC changes and the UHI intensity are studied for the years 2016, 2020, and 2024. The classification of LULC and the extraction of LST (Land surface temperature) are done by analysing Landsat images. The Random Forest machine learning model was used to classify the LULC, for which high accuracy was obtained. By following the split-window algorithm, the LST was calculated by the ArcMap software. UHI Intensity index is also calculated by correlating the LULC and the LST. It measures the relation between the cities and the surrounding rural areas, which in this case, the Forest-Mountain ranges. The prediction for the LULC, LST, and the UHI Intensity was done using the MOULUSCE plugin from the QGIS software. This plugin uses a CA-ANN model to forecast the Land dynamics. It is done by inputting the current conditions along with the other independent variables like slope, DEM, and proximity to roads. The LULC, LST, and the UHI Intensity for 2028 and 2032 were predicted. According to the LULC changes, there has been a steady increase in the urban areas in the study area. The urban areas increased from 14 % to almost 18%, a 4% increase. Similarly, the Fallow lands also increased from 22% to 25%. There is a steady decrease in the Barren Lands, from 35% in 2016 to 29% in 2032. The vegetation was found to be constant throughout the study period, remaining at 16%. The water bodies and the mountain ranges also remained the same. The Land surface temperature experienced some changes. Although the average LST across the years was found to be similar, the area under the $>40^{\circ}\text{C}$ increased from 156 sq. km to 235 sq. km in 2016 to 2032, signalling the rise in surface temperature. The UHI Intensity was found to fluctuate in the study area. The model predicted a rise in area under the “Low” zone, signalling a brief cooling. However, the model also predicted a significant rise in the area under the “High” zone. The phenomenon causes a condition to redistribute heat in other areas rather than alleviating the heat, in other words, amplification of UHI Intensity. The UHI is not only affected by the changes in LULC but also by other factors like climate change, population, building height, vehicular emissions, and other anthropogenic activities. This study provides a basic framework for the government officials, urban planners, and other stakeholders to plan development practices in a more strategic and sustainable. It also provides an understanding to create several mitigation plans, such as promoting green roofing in tall buildings, increasing vegetation cover, especially in barren lands, as it has the highest LST among other land classes.

9. FUTURE PERSPECTIVES

The study can be further developed by incorporating climatic conditions like rainfall, air temperature, and wind speed. Incorporating these factors can further provide valuable input and analysis for stakeholders like urban planners. It can also provide a detailed assessment of how the UHI intensity will respond to these conditions. MODIS and Sentinel images can be used for studying the seasonal variations in the UHI intensity. Both the LST and the UHI intensity can be probed by taking in account of the socio-economic and demographic factors. The UHI intensity is found to be heavily influenced by population, infrastructure and pollution. This can provide a clear understanding of how to mitigate and control its effects. Land Suitability analysis is also an important method by which suitable locations can be identified for increasing vegetation cover, green roofing, cooling pavements, and also the introduction of urban agriculture.

10. REFERENCES

- Akter, T., Gazi, M. Y., & Mia, M. B. (2021). Assessment of Land Cover Dynamics, Land Surface Temperature, and Heat Island Growth in Northwestern Bangladesh Using Satellite Imagery. In *Environmental Processes* (Vol. 8, Issue 2). <https://doi.org/10.1007/s40710-020-00491-y>
- Aneesha Satya, B., Shashi, M., & Deva, P. (2020). Future land use land cover scenario simulation using open source GIS for the city of Warangal, Telangana, India. *Applied Geomatics*, 12(3), 281–290. <https://doi.org/10.1007/s12518-020-00298-4>
- Angel, S., Sheppard, S. C., & Civco, D. L. (2005). The Dynamics of Global Urban Expansion. *The World Bank*, September, 205. http://www.citiesalliance.org/sites/citiesalliance.org/files/CA_Docs/resources/upgrading/urban-expansion/worldbankreportsept2005.pdf
- Aravind, P., Selvakumar, S., Thiagarajan, G., Kannan, B., & Boomiraj, K. (2022). Estimation of land surface temperature for Coimbatore District using Landsat imagery. *Journal of Applied and Natural Science*, 14(SI), 8–15. <https://doi.org/10.31018/jans.v14iSI.3557>
- Aslan, N., & Koc-San, D. (2016). Analysis of relationship between urban heat island effect and Land use/cover type using Landsat 7 ETM+ and Landsat 8 OLI images. *International Archives of the Photogrammetry, Remote Sensing and Spatial Information Sciences - ISPRS Archives*, 41(July), 821–828. <https://doi.org/10.5194/isprsarchives-XLI-B8-821-2016>
- Atasoy, M. (2019). on the Development of Urban Heat Island Effects. *Environment, Development and Sustainability*, 0123456789, 7547–7557. <https://doi.org/10.1007/s10668-019-00535-w>
- Avci, C., Budak, M., Yagmur, N., & Balcik, F. B. (2023). Comparison between random forest and support vector machine algorithms for LULC classification. *International Journal of Engineering and Geosciences*, 8(1), 1–10. <https://doi.org/10.26833/ijeg.987605>
- Bagyaraj, M., Senapathi, V., Karthikeyan, S., Chung, S. Y., Khatibi, R., Nadiri, A. A., & Lajayer, B. A. (2023). A study of urban heat island effects using remote sensing and GIS techniques in Kancheepuram, Tamil Nadu, India. *Urban Climate*, 51, 101597.

- Balsubramanian, G., Pereira, G. F., Swaminathan, B., Goswami, S., & Choudhury, S. B. (2021). *The influence of changes in Land Use/Land Cover (LULC) on Land Surface Temperature in Ramanathapuram coast and Assessment of Urban Heat Island, using remote sensing and GIS*.
- Baniassadi, A., Sailor, D. J., Crank, P. J., & Ban-Weiss, G. A. (2018). Direct and indirect effects of high-albedo roofs on energy consumption and thermal comfort of residential buildings. *Energy and Buildings*, 178, 71–83.
- Cao, H., Liu, J., Chen, J., Gao, J., Wang, G., & Zhang, W. (2019). Spatiotemporal patterns of urban land use change in typical cities in the Greater Mekong Subregion (GMS). *Remote Sensing*, 11(7). <https://doi.org/10.3390/rs11070801>
- Capolupo, A., Monterisi, C., & Tarantino, E. (2020). Landsat Images Classification Algorithm (LICA) to automatically extract land cover information in Google Earth Engine environment. *Remote Sensing*, 12(7), 1201.
- Celik, B., Kaya, S., Alganci, U., Seker, D. Z., & others. (2019). Assessment of the relationship between land use/cover changes and land surface temperatures: a case study of thermal remote sensing. *FEB Fresenius Environ. Bull.*, 3, 541.
- Choudhury, U., Singh, S. K., Kumar, A., Meraj, G., Kumar, P., & Kanga, S. (2023). Assessing Land Use/Land Cover Changes and Urban Heat Island Intensification: A Case Study of Kamrup Metropolitan District, Northeast India (2000–2032). *Earth (Switzerland)*, 4(3), 503–521. <https://doi.org/10.3390/earth4030026>
- Das, T., Jana, A., Mandal, B., & Sutradhar, A. (2022). Spatio-temporal pattern of land use and land cover and its effects on land surface temperature using remote sensing and GIS techniques: a case study of Bhubaneswar city, Eastern India (1991–2021). In *GeoJournal* (Vol. 87, Issue November). Springer Netherlands. <https://doi.org/10.1007/s10708-021-10541-z>
- de Almeida, C. R., Teodoro, A. C., & Gonçalves, A. (2021). Study of the urban heat island (Uhi) using remote sensing data/techniques: A systematic review. *Environments - MDPI*, 8(10), 1–39. <https://doi.org/10.3390/environments8100105>
- Dhar, R. B., Chakraborty, S., Chattopadhyay, R., & Sikdar, P. K. (2019). Impact of Land-Use/Land-Cover Change on Land Surface Temperature Using Satellite Data: A Case

Study of Rajarhat Block, North 24-Parganas District, West Bengal. *Journal of the Indian Society of Remote Sensing*, 47(2), 331–348. <https://doi.org/10.1007/s12524-019-00939-1>

Din, S. U., & Yamamoto, K. (2024). Urban Spatial Dynamics and Geo-informatics Prediction of Karachi from 1990–2050 Using Remote Sensing and CA-ANN Simulation. *Earth Systems and Environment*, 849–868. <https://doi.org/10.1007/s41748-024-00439-4>

Ding, H., & Shi, W. (2013). Land-use/land-cover change and its influence on surface temperature: a case study in Beijing City. *International Journal of Remote Sensing*, 34(15), 5503–5517. <https://doi.org/10.1080/01431161.2013.792966>

Dissanayake, D. M. S. L. B., Morimoto, T., Ranagalage, M., & Murayama, Y. (2019). Land-use/land-cover changes and their impact on surface urban heat islands: Case study of Kandy City, Sri Lanka. *Climate*, 7(8), 1–20. <https://doi.org/10.3390/cli7080099>

Dong, W., Liu, Z., Zhang, L., Tang, Q., Liao, H., & Li, X. (2014). Assessing heat health risk for sustainability in Beijing's urban heat island. *Sustainability (Switzerland)*, 6(10), 7334–7357. <https://doi.org/10.3390/su6107334>

Erdem, U., Cubukcu, K. M., & Sharifi, A. (2021). An analysis of urban form factors driving Urban Heat Island: the case of Izmir. *Environment, Development and Sustainability*, 23(5), 7835–7859. <https://doi.org/10.1007/s10668-020-00950-4>

Faizan, M. (2020). Assessment of Urban Heat Island using GIS and Remote Sensing-A Case Study of Chennai City, India. *Conference: Global to Local Sustainability & Future ... , November.* https://www.researchgate.net/profile/Mohammed-Faizan-2/publication/355814388_Assessment_of_Urban_Heat_Island_using_GIS_and_Remote_Sensing_-A_Case_Study_of_Chennai_City_India/links/617fe2733c987366c3122565/Assessment-of-Urban-Heat-Island-using-GIS-and-Remote-Sensing_-A_Case_Study_of_Chennai_City_India

Faizan, M., & Hudait, M. (2024). *Modelling future land use / land cover and seasonal land surface temperature changes based on CA-ANN algorithm to assess its impacts on Chennai Metropolitan Area (CMA), India 6 th Intercontinental Geoinformation Days Modelling future land use / land cov. January.*

- Fashae, O. A., Adagbasa, E. G., Olusola, A. O., & Obateru, R. O. (2020). Land use/land cover change and land surface temperature of Ibadan and environs, Nigeria. *Environmental Monitoring and Assessment*, 192, 1–18.
- Favretto, A. (2018). *Urban Heat Island analysis with Remote Sensing and GIS methods: an application in the Trieste area (North-East of Italy)*.
- Feng, J.-M., Wang, Y.-L., Ma, Z.-G., & Liu, Y.-H. (2012). Simulating the regional impacts of urbanization and anthropogenic heat release on climate across China. *Journal of Climate*, 25(20), 7187–7203.
- Gantumur, B., Wu, F., Vandansambuu, B., Tsegmid, B., Dalaibaatar, E., & Zhao, Y. (2022). Spatiotemporal dynamics of urban expansion and its simulation using CA-ANN model in Ulaanbaatar, Mongolia. *Geocarto International*, 37(2), 494–509. <https://doi.org/10.1080/10106049.2020.1723714>
- Garuma, G. F. (2022). How the Interaction of Heatwaves and Urban Heat Islands Amplify Urban Warming. *Advances in Environmental and Engineering Research*, 3(2), 1–1. <https://doi.org/10.21926/aeer.2202022>
- Ghosh, J., & Porchelvan, P. (2018). *Relationship Between Surface Temperature and Land Cover Types Using Thermal Infrared Band and NDVI for Vellore District, Tamilnadu, India Nature Environment and Pollution Technology An International Quarterly Scientific Journal Open Access*. 17(2008), 611–617. www.neptjournal.com
- Giniyatullina, O. L., Potapov, V. P., & Schastlivtsev, E. L. (2014). Integral methods of environmental assessment at mining regions based on remote sensing data. *International Journal of Engineering and Innovative Technology*, 4(4), 220–224.
- Gogoi, P. P., Vinoj, V., Swain, D., Roberts, G., Dash, J., & Tripathy, S. (2019). Land use and land cover change effect on surface temperature over Eastern India. *Scientific Reports*, 9(1), 1–10. <https://doi.org/10.1038/s41598-019-45213-z>
- Grifoni, R. C., Passerini, G., & Pierantozzi, M. (2013). Assessment of outdoor thermal comfort and its relation to urban geometry. *WIT Transactions on Ecology and the Environment*, 173, 3–14. <https://doi.org/10.2495/SDP130011>

- Guha, S., Govil, H., Gill, N., & Dey, A. (2020). Analytical study on the relationship between land surface temperature and land use/land cover indices. *Annals of GIS*, 26(2), 201–216. <https://doi.org/10.1080/19475683.2020.1754291>
- Gupta, N., Mathew, A., & Khandelwal, S. (2020). Spatio-temporal impact assessment of land use / land cover (LU-LC) change on land surface temperatures over Jaipur city in India. *International Journal of Urban Sustainable Development*, 12(3), 283–299. <https://doi.org/10.1080/19463138.2020.1727908>
- Han, D., Zhang, T., Qin, Y., Tan, Y., & Liu, J. (2023). A comparative review on the mitigation strategies of urban heat island (UHI): a pathway for sustainable urban development. *Climate and Development*, 15(5), 379–403. <https://doi.org/10.1080/17565529.2022.2092051>
- Harmay, N. S. M., Kim, D., & Choi, M. (2021). Urban heat island associated with land use/land cover and climate variations in Melbourne, Australia. *Sustainable Cities and Society*, 69, 102861.
- Hayes, A. T., Jandaghian, Z., Lacasse, M. A., Gaur, A., Lu, H., Laouadi, A., Ge, H., & Wang, L. (2022). Nature-Based Solutions (NBSs) to Mitigate Urban Heat Island (UHI) Effects in Canadian Cities. *Buildings*, 12(7). <https://doi.org/10.3390/buildings12070925>
- Heaviside, C., Macintyre, H., & Vardoulakis, S. (2017). The Urban Heat Island: Implications for Health in a Changing Environment. *Current Environmental Health Reports*, 4(3), 296–305. <https://doi.org/10.1007/s40572-017-0150-3>
- Heisler, G. M., & Brazel, A. J. (2015). The urban physical environment: Temperature and urban heat islands. *Urban Ecosystem Ecology*, 13210, 29–56. <https://doi.org/10.2134/agronmonogr55.c2>
- Hu, L., & Brunsell, N. A. (2015). A new perspective to assess the urban heat island through remotely sensed atmospheric profiles. *Remote Sensing of Environment*, 158, 393–406. <https://doi.org/10.1016/j.rse.2014.10.022>
- Ibrahim, G. R. F. (2017). Urban land use land cover changes and their effect on land surface temperature: Case study using Dohuk City in the Kurdistan Region of Iraq. *Climate*, 5(1). <https://doi.org/10.3390/cli5010013>

- Jiang, J., & Tian, G. (2010). Analysis of the impact of Land use/Land cover change on Land Surface Temperature with Remote Sensing. *Procedia Environmental Sciences*, 2(5), 571–575. <https://doi.org/10.1016/j.proenv.2010.10.062>
- Kafy, A. Al, Faisal, A. Al, Al Rakib, A., Roy, S., Ferdousi, J., Raikwar, V., Kona, M. A., & Fatin, S. M. A. Al. (2021). Predicting changes in land use/land cover and seasonal land surface temperature using multi-temporal landsat images in the northwest region of Bangladesh. *Heliyon*, 7(7). <https://doi.org/10.1016/j.heliyon.2021.e07623>
- Karakuş, C. B. (2019). The Impact of Land Use/Land Cover (LULC) Changes on Land Surface Temperature in Sivas City Center and Its Surroundings and Assessment of Urban Heat Island. *Asia-Pacific Journal of Atmospheric Sciences*, 55(4), 669–684. <https://doi.org/10.1007/s13143-019-00109-w>
- Kasahun, M., & Legesse, A. (2024). Machine learning for urban land use/ cover mapping: Comparison of artificial neural network, random forest and support vector machine, a case study of Dilla town. *Heliyon*, 10(20), e39146. <https://doi.org/10.1016/j.heliyon.2024.e39146>
- Khan, M. S., Ullah, S., Sun, T., Rehman, A. U., & Chen, L. (2020). Land-use/land-cover changes and its contribution to urban heat Island: A case study of Islamabad, Pakistan. *Sustainability (Switzerland)*, 12(9). <https://doi.org/10.3390/su12093861>
- Kikon, N., Singh, P., Singh, S. K., & Vyas, A. (2016). Assessment of urban heat islands (UHI) of Noida City, India using multi-temporal satellite data. *Sustainable Cities and Society*, 22, 19–28. <https://doi.org/10.1016/j.scs.2016.01.005>
- Knorn, J., Rabe, A., Radeloff, V. C., Kuemmerle, T., Kozak, J., & Hostert, P. (2009). Land cover mapping of large areas using chain classification of neighboring Landsat satellite images. *Remote Sensing of Environment*, 113(5), 957–964. <https://doi.org/10.1016/j.rse.2009.01.010>
- Koç, A., Caf, A., Koç, C., & Kejanli, D. T. (2022). Examining the temporal and spatial distribution of potential urban heat island formations. *Environmental Science and Pollution Research*, 29(8), 11455–11468. <https://doi.org/10.1007/s11356-021-16422-9>
- Kubilay, A., Allegrini, J., Strelbel, D., Zhao, Y., Derome, D., & Carmeliet, J. (2020). Advancement in urban climate modelling at local scale: Urban heat island mitigation

and building cooling demand. *Atmosphere*, 11(12), 1–20.
<https://doi.org/10.3390/atmos11121313>

Kulithalai Shiyam Sundar, P., & Deka, P. C. (2022). Spatio-temporal classification and prediction of land use and land cover change for the Vembanad Lake system, Kerala: a machine learning approach. *Environmental Science and Pollution Research*, 29(57), 86220–86236. <https://doi.org/10.1007/s11356-021-17257-0>

Lambin, E. F., Geist, H. J., & Lepers, E. (2003). Dynamics of land-use and land-cover change in tropical regions. *Annual Review of Environment and Resources*, 28(January 2003), 205–241. <https://doi.org/10.1146/annurev.energy.28.050302.105459>

Lee, Y. Y., Md Din, M. F., Ponraj, M., Noor, Z. Z., Iwao, K., & Chelliapan, S. (2017). Overview of Urban Heat Island (UHI) phenomenon towards human thermal comfort. *Environmental Engineering and Management Journal*, 16(9), 2097–2112. <https://doi.org/10.30638/eemj.2017.217>

Li, C., & Zhang, N. (2021). Analysis of the Daytime Urban Heat Island Mechanism in East China. *Journal of Geophysical Research: Atmospheres*, 126(12), 1–19. <https://doi.org/10.1029/2020JD034066>

Li, X., Zhou, Y., Yu, S., Jia, G., Li, H., & Li, W. (2019). Urban heat island impacts on building energy consumption: A review of approaches and findings. *Energy*, 174(515), 407–419. <https://doi.org/10.1016/j.energy.2019.02.183>

Li, Y., Schubert, S., Kropp, J. P., & Rybski, D. (2020). On the influence of density and morphology on the Urban Heat Island intensity. *Nature Communications*, 11(1), 1–9. <https://doi.org/10.1038/s41467-020-16461-9>

Liapopoulou, E., & Heo, Y. (2013). *The Effect of Urban Geometry on Microclimate*. Department of Engineering, University of Cambridge, Cambridge, UK School of Civil, Environmental and Architectural Engineering, Korea University, Seoul, Korea. 777–784.

Liu, P., Jia, S., Han, R., Liu, Y., Lu, X., & Zhang, H. (2020). RS and GIS Supported Urban LULC and UHI Change Simulation and Assessment. *Journal of Sensors*, 2020. <https://doi.org/10.1155/2020/5863164>

- Liu, R., & Han, Z. (2016). The Effects of Anthropogenic Heat Release on Urban Meteorology and Implication for Haze Pollution in the Beijing-Tianjin-Hebei Region. *Advances in Meteorology*, 2016. <https://doi.org/10.1155/2016/6178308>
- Liu, X., Liang, X., Li, X., Xu, X., Ou, J., Chen, Y., Li, S., Wang, S., & Pei, F. (2017). A future land use simulation model (FLUS) for simulating multiple land use scenarios by coupling human and natural effects. *Landscape and Urban Planning*, 168(September), 94–116. <https://doi.org/10.1016/j.landurbplan.2017.09.019>
- Loughnan, M., Nicholls, N., & Tapper, N. J. (2012). Mapping Heat Health Risks in Urban Areas. *International Journal of Population Research*, 2012, 1–12. <https://doi.org/10.1155/2012/518687>
- Manteghi, G. (2020). *International Transaction Journal of Engineering , Management , & Applied Sciences & Technologies EVAPORATIVE PAVEMENTS AS AN URBAN HEAT ISLAND (UHI) MITIGATION STRATEGY: A REVIEW*. 11(1), 1–15. <https://doi.org/10.14456/ITJEMAST.2020.17>
- Marianne Rhea, R., & Thangaperumal, S. (2023). Spatio-Temporal Analysis of Urbanization by Using Supervised Image Classification with Correlation of Land Surface Temperature and Topography. *Proceedings of International Conference on Data Science and Applications: ICDSA 2022, Volume 2*, 369–395.
- Martin-Vide, J., Sarricolea, P., & Moreno-García, M. C. (2015). On the definition of urban heat island intensity: The “rural” reference. *Frontiers in Earth Science*, 3(June), 2–4. <https://doi.org/10.3389/feart.2015.00024>
- Mas, J. F. (1999). Monitoring land-cover changes: A comparison of change detection techniques. *International Journal of Remote Sensing*, 20(1), 139–152. <https://doi.org/10.1080/014311699213659>
- Merbitz, H., Buttstädt, M., Michael, S., Dott, W., & Schneider, C. (2012). GIS-based identification of spatial variables enhancing heat and poor air quality in urban areas. *Applied Geography*, 33(1), 94–106. <https://doi.org/10.1016/j.apgeog.2011.06.008>
- Mishra, O., Khatiwada, N., Joshi, D., Gharti, S., & Khatri, B. (2024). *Prediction of Land Use Land Cover Change Using a Coupled CA-ANN modeling in Dhanusha district of Nepal*.

- Moazzam, M. F. U., Doh, Y. H., & Lee, B. G. (2022). Impact of urbanization on land surface temperature and surface urban heat Island using optical remote sensing data: A case study of Jeju Island, Republic of Korea. In *Building and Environment* (Vol. 222). <https://doi.org/10.1016/j.buildenv.2022.109368>
- Moghbel, M., & Shamsipour, A. A. (2019). Spatiotemporal characteristics of urban land surface temperature and UHI formation: a case study of Tehran, Iran. *Theoretical and Applied Climatology*, 137(3–4), 2463–2476. <https://doi.org/10.1007/s00704-018-2735-7>
- Mohajerani, A., Bakaric, J., & Jeffrey-Bailey, T. (2017). The urban heat island effect, its causes, and mitigation, with reference to the thermal properties of asphalt concrete. *Journal of Environmental Management*, 197, 522–538. <https://doi.org/10.1016/j.jenvman.2017.03.095>
- Mohammad, P., Goswami, A., Chauhan, S., & Nayak, S. (2022). Machine learning algorithm based prediction of land use land cover and land surface temperature changes to characterize the surface urban heat island phenomena over Ahmedabad city, India. *Urban Climate*, 42(October 2023). <https://doi.org/10.1016/j.uclim.2022.101116>
- Mohan, M., & Kandya, A. (2015). Impact of urbanization and land-use/land-cover change on diurnal temperature range: A case study of tropical urban airshed of India using remote sensing data. *Science of the Total Environment*, 506–507, 453–465. <https://doi.org/10.1016/j.scitotenv.2014.11.006>
- Mohan, M., Kikegawa, Y., Gurjar, B. R., Bhati, S., & Kolli, N. R. (2013). Assessment of urban heat island effect for different land use-land cover from micrometeorological measurements and remote sensing data for megacity Delhi. *Theoretical and Applied Climatology*, 112(3–4), 647–658. <https://doi.org/10.1007/s00704-012-0758-z>
- Morris, K. I., Chan, A., Morris, K. J. K., Ooi, M. C. G., Oozeer, M. Y., Abakr, Y. A., Nadzir, M. S. M., Mohammed, I. Y., & Al-Qrimli, H. F. (2017). Impact of urbanization level on the interactions of urban area, the urban climate, and human thermal comfort. *Applied Geography*, 79, 50–72. <https://doi.org/10.1016/j.apgeog.2016.12.007>
- Muthiah, K., Mathivanan, M., & Duraisekaran, E. (2022). Dynamics of urban sprawl on the peri-urban landscape and its relationship with urban heat island in Chennai Metropolitan Area, India. *Arabian Journal of Geosciences*, 15(23). <https://doi.org/10.1007/s12517-022-10959-w>

- Nakata-Osaki, C. M., De Souza, L. C. L., & Rodrigues, D. S. (2015). A GIS extension model to calculate urban heat island intensity based on urban geometry. *CUPUM 2015 - 14th International Conference on Computers in Urban Planning and Urban Management*.
- Narayani, A. R., & Nagalakshmi, R. (2024). *Investigating the Link Between Urban Expansion and Land Surface Temperature using GIS and Spectral Indices . The case of Peri urban South Chennai*. 16.
- Nuruzzaman, Md. (2015). Urban Heat Island: Causes, Effects and Mitigation Measures - A Review. *International Journal of Environmental Monitoring and Analysis*, 3(2), 67. <https://doi.org/10.11648/j.ijema.20150302.15>
- Oleson, K. W., Monaghan, A., Wilhelmi, O., Barlage, M., Brunsell, N., Feddema, J., Hu, L., & Steinhoff, D. F. (2015). Interactions between urbanization, heat stress, and climate change. *Climatic Change*, 129(3–4), 525–541. <https://doi.org/10.1007/s10584-013-0936-8>
- O’Malley C., P. P. A. F. E. R. & G. J. (2014). *An investigation into minimizing urban heat island (UHI) effects: A UK perspective*.
- Palanisamy, M., Balasubramaniam, P., & Periasamy, T. (n.d.). *MODELLING URBAN HEAT ISLAND USING REMOTE SENSING INDICES IN TIRUPPUR MUNICIPAL CORPORATION, TAMIL NADU*.
- Peng, J., Ma, J., Liu, Q., Liu, Y., Hu, Y., Li, Y., & Yue, Y. (2018). Spatial-temporal change of land surface temperature across 285 cities in China: An urban-rural contrast perspective. *Science of the Total Environment*, 635, 487–497.
- Pramanik, S., & Punia, M. (2020). Land use/land cover change and surface urban heat island intensity: source–sink landscape-based study in Delhi, India. *Environment, Development and Sustainability*, 22(8), 7331–7356. <https://doi.org/10.1007/s10668-019-00515-0>
- Rajeshwari, A., & Mani, N. D. (2014). Estimation of land surface temperature of Dindigul district using Landsat 8 data. *International Journal of Research in Engineering and Technology*, 3(5), 122–126.

- Rees, G., Hebry-Baidy, L., & Belenok, V. (2024). Temporal variations in land surface temperature within an urban ecosystem: A comprehensive assessment of land use and land cover change in Kharkiv, Ukraine. *Remote Sensing*, 16(9), 1637.
- Rendana, M., Idris, W. M. R., Rahim, S. A., Abdo, H. G., Almohamad, H., Al Dughairi, A. A., & Al-Mutiry, M. (2023). Relationships between land use types and urban heat island intensity in Hulu Langat district, Selangor, Malaysia. *Ecological Processes*, 12(1). <https://doi.org/10.1186/s13717-023-00446-9>
- Rousta, I., Sarif, M. O., Gupta, R. D., Olafsson, H., Ranagalage, M., Murayama, Y., Zhang, H., & Mushore, T. D. (2018). Spatiotemporal analysis of land use/land cover and its effects on surface urban heat Island using landsat data: A case study of Metropolitan City Tehran (1988-2018). *Sustainability (Switzerland)*, 10(12). <https://doi.org/10.3390/su10124433>
- Sachindra, D. A., Ng, A. W. M., Muthukumaran, S., & Perera, B. J. C. (2016). Impact of climate change on urban heat island effect and extreme temperatures: A case-study. *Quarterly Journal of the Royal Meteorological Society*, 142(694), 172–186. <https://doi.org/10.1002/qj.2642>
- Sameh, S., Zarzoura, F., & El-Mewafi, M. (2022). Automated Mapping of Urban Heat Island to Predict Land Surface Temperature and Land Use/Cover Change Using Machine Learning Algorithms: Mansoura City. *International Journal of Geoinformatics*, 18(6), 47–67. <https://doi.org/10.52939/ijg.v18i6.2461>
- Schulp, C. J. E., Nabuurs, G.-J., & Verburg, P. H. (2008). Future carbon sequestration in Europe—effects of land use change. *Agriculture, Ecosystems & Environment*, 127(3–4), 251–264.
- Shahmohamadi, P., Che-Ani, A. I., Etessam, I., Maulud, K. N. A., & Tawil, N. M. (2011). Healthy environment: The need to mitigate urban heat island effects on human health. *Procedia Engineering*, 20, 61–70. <https://doi.org/10.1016/j.proeng.2011.11.139>
- Shahmohamadi, P., Che-Ani, A. I., Maulud, K. N. A., Tawil, N. M., & Abdullah, N. A. G. (2011). The Impact of Anthropogenic Heat on Formation of Urban Heat Island and Energy Consumption Balance. *Urban Studies Research*, 2011(1). <https://doi.org/10.1155/2011/497524>

- Shahmohamadi, P., Che-Ani, A. I., Ramly, A., Maulud, K. N. A., & Mohd-Nor, M. F. I. (2010). Reducing urban heat island effects: A systematic review to achieve energy consumption balance. *International Journal of Physical Sciences*, 5(6), 626–636.
- Shi, L., Luo, Z., Matthews, W., Wang, Z., Li, Y., & Liu, J. (2019). Impacts of urban microclimate on summertime sensible and latent energy demand for cooling in residential buildings of Hong Kong. *Energy*, 189. <https://doi.org/10.1016/j.energy.2019.116208>
- Small, G., Jimenez, I., Salzl, M., & Shrestha, P. (2020). Urban heat island mitigation due to enhanced evapotranspiration in an urban garden in saint paul, minnesota, usa. *WIT Transactions on Ecology and the Environment*, 243, 39–45. <https://doi.org/10.2495/UA200041>
- Swamy, G., Shiva Nagendra, S. M., & Schlink, U. (2017). Urban Heat Island (UHI) influence on secondary pollutant formation in a tropical humid environment. *Journal of the Air and Waste Management Association*, 67(10), 1080–1091. <https://doi.org/10.1080/10962247.2017.1325417>
- Talukdar, S., Singha, P., Mahato, S., Pal, S., Liou, Y. A., & Rahman, A. (2020). Land-use land-cover classification by machine learning classifiers for satellite observations—A review. *Remote sensing*, 12(7), 1135.
- Tan, J., Zheng, Y., Tang, X., Guo, C., Li, L., Song, G., Zhen, X., Yuan, D., Kalkstein, A. J., Li, F., & Chen, H. (2010). The urban heat island and its impact on heat waves and human health in Shanghai. *International Journal of Biometeorology*, 54(1), 75–84. <https://doi.org/10.1007/s00484-009-0256-x>
- Taslim, S., Parapari, D. M., & Shafaghat, A. (2015). Jurnal Teknologi Full paper Urban Design Guidelines to Mitigate Urban Heat Island (UHI) Effects In Hot-. *Jurnal Teknologi*, 4(7), 119–124.
- Tewari, M., Salamanca, F., Martilli, A., Treinish, L., & Mahalov, A. (2017). Impacts of projected urban expansion and global warming on cooling energy demand over a semiarid region. *Atmospheric Science Letters*, 18(11), 419–426. <https://doi.org/10.1002/asl.784>

- Thonfeld, F., Steinbach, S., Muro, J., & Kirimi, F. (2020). Long-term land use/land cover change assessment of the Kilombero catchment in Tanzania using random forest classification and robust change vector analysis. *Remote Sensing*, 12(7). <https://doi.org/10.3390/rs12071057>
- Tran, D. X., Pla, F., Latorre-Carmona, P., Myint, S. W., Caetano, M., & Kieu, H. V. (2017). Characterizing the relationship between land use land cover change and land surface temperature. *ISPRS Journal of Photogrammetry and Remote Sensing*, 124, 119–132. <https://doi.org/10.1016/j.isprsjprs.2017.01.001>
- Vardoulakis, E., Karamanis, D., Fotiadi, A., & Mihalakakou, G. (2013). The urban heat island effect in a small Mediterranean city of high summer temperatures and cooling energy demands. *Solar Energy*, 94, 128–144. <https://doi.org/10.1016/j.solener.2013.04.016>
- Verburg, P. H., Neumann, K., & Nol, L. (2011). Challenges in using land use and land cover data for global change studies. *Global Change Biology*, 17(2), 974–989. <https://doi.org/10.1111/j.1365-2486.2010.02307.x>
- Verma, R., & Garg, P. K. (2021). Mapping the Spatiotemporal Changes of Land Use/Land Cover on the Urban Heat Island Effect by Open Source Data: A Case Study of Lucknow, India. *Journal of the Indian Society of Remote Sensing*, 49(11), 2655–2671. <https://doi.org/10.1007/s12524-021-01421-7>
- Vohra, R., Kumar, A., Jain, R., & Hemanth, D. J. (2024). Analysis and prediction of land surface temperature with increasing urbanisation using satellite imagery. *Heliyon*, 10(22), e40378. <https://doi.org/10.1016/j.heliyon.2024.e40378>
- Voogt, J. A., & Oke, T. R. (2003). Thermal remote sensing of urban climates. *Remote Sensing of Environment*, 86(3), 370–384. [https://doi.org/10.1016/S0034-4257\(03\)00079-8](https://doi.org/10.1016/S0034-4257(03)00079-8)
- Xiang, X., Zhai, Z., Fan, C., Ding, Y., Ye, L., & Li, J. (2024). Modelling future land use land cover changes and their impacts on urban heat island intensity in Guangzhou, China. *Journal of Environmental Management*, 366, 121787.
- Yang, B., Meng, F., Ke, X., & Ma, C. (2015). The impact analysis of water body landscape pattern on urban heat Island: A case study of Wuhan city. *Advances in Meteorology*, 2015. <https://doi.org/10.1155/2015/416728>

- Yang, J., Wang, Z. H., & Kaloush, K. E. (2015). Environmental impacts of reflective materials: Is high albedo a “silver bullet” for mitigating urban heat island? *Renewable and Sustainable Energy Reviews*, 47, 830–843. <https://doi.org/10.1016/j.rser.2015.03.092>
- Yi, C. Y., & Peng, C. (2017). Correlating cooling energy use with urban microclimate data for projecting future peak cooling energy demands: Residential neighbourhoods in Seoul. *Sustainable Cities and Society*, 35, 645–659.
- Zhang, D. L., Shou, Y. X., & Dickerson, R. R. (2009). Upstream urbanization exacerbates urban heat island effects. *Geophysical Research Letters*, 36(24), 1–5. <https://doi.org/10.1029/2009GL041082>
- Zhao, Z., Islam, F., Waseem, L. A., Tariq, A., Nawaz, M., Islam, I. U., Bibi, T., Rehman, N. U., Ahmad, W., Aslam, R. W., Raza, D., & Hatamleh, W. A. (2024). Comparison of Three Machine Learning Algorithms Using Google Earth Engine for Land Use Land Cover Classification. *Rangeland Ecology and Management*, 92(December), 129–137. <https://doi.org/10.1016/j.rama.2023.10.007>
- Zhou, D., Zhao, S., Liu, S., Zhang, L., & Zhu, C. (2014). Surface urban heat island in China’s 32 major cities: Spatial patterns and drivers. *Remote Sensing of Environment*, 152, 51–61. <https://doi.org/10.1016/j.rse.2014.05.017>
- Zipper, S. C., Schatz, J., Kucharik, C. J., & Loheide, S. P. (2017). Urban heat island-induced increases in evapotranspirative demand. *Geophysical Research Letters*, 44(2), 873–881. <https://doi.org/10.1002/2016GL072190>
- Zipper, S. C., Schatz, J., Singh, A., Kucharik, C. J., Townsend, P. A., & Loheide, S. P. (2016). Urban heat island impacts on plant phenology: Intra-urban variability and response to land cover. *Environmental Research Letters*, 11(5). <https://doi.org/10.1088/1748-9326/11/5/054023>